

AD-A193 058

INVESTIGATION OF THE SUN-ALIGNED F-ALIGNED F-REGION  
WALLS AND RELATED PHE. (U) SWEDISH INST OF SPACE  
PHYSICS KIRUNA A STEEN 21 JUL 87 AFGL-TR-87-0248

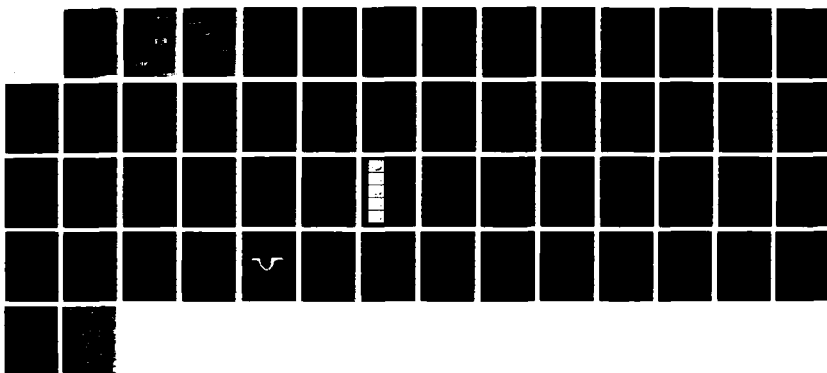
1/1

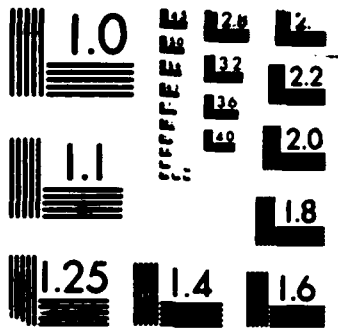
UNCLASSIFIED

XAFOSR-84-0084

F/G 4/1

NL





MICROCOPY RESOLUTION TEST CHART  
JAN 40 STANARDS 1963 A

AD-A193 858

AFGL-TR-87-0248

2  
DTIC FILE COPY

INVESTIGATION OF THE SUN-ALIGNED F-REGION WALLS  
AND RELATED PHENOMENA IN THE AURORAL LATITUDE  
RANGE.

Ake Steen  
Swedish Institute of Space Physics  
P.O. Box 812, S-901 28 KIRUNA  
SWEDEN

21 July 1987

DTIC  
SELECTED  
MAY 06 1988  
S D  
4 D

Final Report  
1 March 1986 - 28 February 1987

Approved for public release;  
distribution unlimited

AIR FORCE GEOPHYSICAL RESEARCH  
AIR FORCE GEOPHYSICAL RESEARCH  
DIVISION OF THE AIR FORCE  
RESEARCH LABORATORY

"This technical report has been reviewed and is approved for publication."



EDWARD J. WEBER  
Contract Manager



HERBERT C. CARLSON, Jr.  
Branch Chief

FOR THE COMMANDER



ROBERT A. SKRAWEK  
Division Director

This document has been reviewed by the ESD Public Affairs Office (PA) and is releasable to the National Technical Information Service (NTIS).

Qualified requestors may obtain additional copies from the Defense Technical Information Center. All others should apply to the National Technical Information Service.

If your address has changed, or if you wish to be removed from the mailing list, or if the addressee is no longer employed by your organization, please notify AFGL/DAA, Hanscom AFB, MA 01731. This will assist us in maintaining a current mailing list.

Do not return copies of this report unless contractual obligations or notices on a specific document requires that it be returned.

Unclassified

SECURITY CLASSIFICATION OF THIS PAGE

REPORT DOCUMENTATION PAGE

1a. REPORT SECURITY CLASSIFICATION Unclassified		1b. RESTRICTIVE MARKINGS										
2a. SECURITY CLASSIFICATION AUTHORITY Public Law 97 - 258		3. DISTRIBUTION/AVAILABILITY OF REPORT Approved for public release, distribution unlimited										
2b. DECLASSIFICATION/DOWNGRADING SCHEDULE												
4. PERFORMING ORGANIZATION REPORT NUMBER(S)		5. MONITORING ORGANIZATION REPORT NUMBER(S) AFGL-TR-87-0248										
6a. NAME OF PERFORMING ORGANIZATION Swedish Institute of Space Physics	6b. OFFICE SYMBOL IRF	7a. NAME OF MONITORING ORGANIZATION Air Force Office of Scientific Research										
8c. ADDRESS (City, State and ZIP Code) P.O. Box 812 S-981 28 KIRUNA, SWEDEN		7b. ADDRESS (City, State and ZIP Code) AFOSR/PKZ Building 410, Bolling AFB, DC 20332, USA										
9a. NAME OF FUNDING/SPONSORING ORGANIZATION EOARD	9b. OFFICE SYMBOL (If applicable)	10. PROCUREMENT INSTRUMENT IDENTIFICATION NUMBER AFOSR-84-0084 C										
11c. ADDRESS (City, State and ZIP Code) 223/231 Old Marylebone Rd LONDON NW1 5TH, UK		10. SOURCE OF FUNDING NOS. <table border="1"><tr><td>PROGRAM ELEMENT NO.</td><td>PROJECT NO.</td><td>TASK NO.</td><td>WORK UNIT NO.</td></tr><tr><td>62101F</td><td>4643</td><td>09</td><td>AE</td></tr></table>		PROGRAM ELEMENT NO.	PROJECT NO.	TASK NO.	WORK UNIT NO.	62101F	4643	09	AE	
PROGRAM ELEMENT NO.	PROJECT NO.	TASK NO.	WORK UNIT NO.									
62101F	4643	09	AE									
11. TITLE (Include Security Classification) Investigation of the Sun-Aligned F-Region Walls and Related	12. PERSONAL AUTHOR(S) Phenomena in the Auroral Latitude Range Steen, Ake											
13a. TYPE OF REPORT Final Scientific	13b. TIME COVERED FROM 860301 TO 870228	14. DATE OF REPORT (Yr., Mo., Day) 1987-07-21	15. PAGE COUNT 58									
16. SUPPLEMENTARY NOTATION												
17. COGATI CODES <table border="1"><tr><td>FIELD</td><td>GROUP</td><td>SUB. GR.</td></tr><tr><td></td><td></td><td></td></tr><tr><td></td><td></td><td></td></tr></table>	FIELD	GROUP	SUB. GR.							18. SUBJECT TERMS (Continue on reverse if necessary and identify by block number) Aurora, ground based optical instruments, coordinated observations, EISCAT, HILAT, VIKING		
FIELD	GROUP	SUB. GR.										
19. ABSTRACT (Continue on reverse if necessary and identify by block number) The final scientific report describes the research activities in Kiruna utilizing ground-based optical equipment, incoherent scatter radar, VIKING and HILAT satellites for the study of auroral processes. The development work of the optical instrumentation is summarized, and the current scientific work is reviewed. (See page 2)												
20. DISTRIBUTION/AVAILABILITY OF ABSTRACT UNCLASSIFIED/UNLIMITED <input checked="" type="checkbox"/> SAME AS RPT. <input type="checkbox"/> DTIC USERS <input type="checkbox"/>		21. ABSTRACT SECURITY CLASSIFICATION Unclassified										
22a. NAME OF RESPONSIBLE INDIVIDUAL Edward Weber		22b. TELEPHONE NUMBER (Include Area Code) (617) 377-3121	22c. OFFICE SYMBOL AFGL/LIS									

DD FORM 1473, 83 APR

EDITION OF 1 JAN 73 IS OBSOLETE.

Unclassified  
SECURITY CLASSIFICATION OF THIS PAGE

i/ii

TABLE OF CONTENTS

	page
1. Summary of the optical auroral research work	1
2. References	3
Appendix 1	5
Appendix 2	44
Appendix 3	45
Appendix 4	49

Accession For	
NTIS CRA&I	<input checked="" type="checkbox"/>
DTIC TAB	<input type="checkbox"/>
Unannounced	<input type="checkbox"/>
Justification	
By	
Distribution	
Availability Codes	
Dist	Avail And/or Special
A-1	

DTIC  
COPY  
INSPECTED  
4

## 1. Summary of the optical auroral research work

The period March 1986 to the end of fall 1986 was very much characterized by activities related to the swedish satellite VIKING. The optical program in Kiruna was focused on ground-based measurement campaigns and on an optical experiment carried by one of the rockets in the AURELD-VIP project. In addition a new optical laboratory was completed during the summer months of 1986. However, as a result of a change in the science policy for the optical program at the institute in Kiruna, the activities during the spring 1987 have almost entirely been directed towards scientific work, causing a drastic reduction in the efforts which normally are used for new hardware developments and for new measurement programs.

A submitted study of an eastward drifting fold in an auroral arc (Steen et al., 1987), included data from a HILAT pass, and is shown in appendix 1. A phase 1 analysis of the data from the new optical rocket experiment has been published as conference proceedings (Sandahl et al., 1987; Rees and Steen, 1987). Appendix 2 shows that the one-dimensional imaging detector very nicely probes the E-region both on upleg and downleg. In a joint swedish-canadian study (Shepherd et al., 1987), using data from the VIKING UV-imager and data from the ground-based bistatic meridian measuring array (HMS), several interesting phenomena have been observed.

Appendix 3 shows an event from that study during which large-scale oscillation (in the minute range) of the auroral oval is observed both from ground and from space. The final submission of that work will take place in the fall of 1987.

The new optical laboratory at the institute has been described in a technical report (Steen, 1987). A shorter version will appear in the IAGA News in November this year (Appendix 4).

Recent scientific publications from the neutral wind measurement program include a study of data from a six years period to establish the avarage neutral wind pattern (Rees et al., 1987). In a study using the meridional neutral wind data and global auroral information (such as VIKING images) the exact timing between the substorm onset and a discovered reduction in the meridional wind is discussed (Steen and Rees, 1987).

In summary the third year of the 3-year AFOSR-contract has been devoted to measurement campaigns during the VIKING-period and intensified efforts on scientific publications.

Together with the two previously written interim scientific reports this constitute the final scientific report.

## 2. References

- Rees, D., N.D. Lloyd, T.J. Fuller-Rowell, and Å. Steen, Variations of thermospheric winds in Northern Scandinavia between 1980 and 1986: A study of geomagnetic activity effects during the last solar cycle, *Geophysical Surveys*, 9, 1987.
- Rees, D., and Å. Steen, A new technique for rocket and spaceborne investigations of time-dependent auroral morphology, *Proceeding ESA-meeting, Sunne, Sweden, 1987.*
- Sandahl, I., Å. Steen, A. Pellinen-Wannberg, F. Søraas, and J.S. Murphree, First results from the VIKING associated AURELD-VIP rocket and EISCAT campaign, *Proceedings ESA-meeting, Sunne, Sweden, 1987.*
- Shepherd, G.G., Å. Steen, J.S. Murphree, C.D. Anger, and D. Rees, Simultaneous auroral observations from the VIKING spacecraft and from the ground, *Submission to Pl. Space Sci. in the fall 1987.*
- Steen, Å., The optical laboratory in Kiruna: A new research facility in the auroral zone, *KGI Technical Report 033, February 1987.*
- Steen, Å., P.N. Collis, and I. Häggström, On the development of folds in auroral arcs, *submitted to JATP, 1987.*
- Steen, Å., and D. Rees, Discussion on the relation between the neutral wind and auroral intensifications. *In-preparation for publication.*

ON THE DEVELOPMENT OF FOLDS IN AURORAL ARCS

by

1)                  2)                  1)  
A. Steen , P.N. Collis, and I. Häggström

1)  
Swedish Institute of Space Physics  
P.O. Box 812, S-981 28 Kiruna, Sweden

2)  
EISCAT Scientific Association  
P.O. Box 812, S-981 28 Kiruna, Sweden

## ABSTRACT

The development of an auroral arc in the midnight sector from diffuse to discrete with subsequent large scale folding, is studied with the aid of several ground-based observations, including incoherent scatter data, and data from a HILAT satellite pass. Ion drift velocities in the F-region, as measured by EISCAT, were consistently eastward throughout and after the whole period of development, whilst the ion temperature showed two large enhancements just prior to the appearance of the main auroral fold. The fold moved eastwards and crossed the EISCAT antenna beam, appearing as a short-lived spike in electron density at altitudes between about 100 km and 400 km. The spike in electron density came progressively later at higher altitudes. The observations are interpreted as the result of enhanced convection in the ionosphere and in the magnetosphere. The auroral arc folding is suggested to be caused by the Kelvin-Helmholtz instability in a velocity shear zone in the magnetosphere.

## INTRODUCTION

Perturbations of stable auroral arcs, of diffuse or discrete type, are common phenomena. The perturbations most frequently occur during the expansion and recovery phases of the substorm. A well-known, but poorly understood, perturbation is the westward travelling surge, WTS, (Akasofu et al., 1966; Steen and Gustafsson, 1981) which is initiated close to the midnight meridian with a following expansion, predominantly westward. On the dawn side of the midnight meridian the perturbations have acquired different names. Torches and omega bands (Akasofu and Kimball, 1964; Steen and Rees, 1983) are undulations, of different size, of the poleward border of the oval. They drift eastward with a speed in the range  $400\text{-}2000\text{ ms}^{-1}$ . Folds in auroral arcs and auroral spirals have been reported to occur on the dawn side as well as on the evening side (Davis and Hallinan, 1976). Instead of a drift speed the auroral spirals and folds have a rotational speed connected with them during the formation. A rotational speed of  $900\text{ ms}^{-1}$  (Akasofu and Kimball, 1964) in one case and several tens of  $\text{kms}^{-1}$  (Oguti, 1974) in another case, have been reported. In the search for theoretical explanations, different mechanisms have been investigated which could cause an instability to develop from an original stable situation (stable arc or diffuse auroral oval). Instabilities responsible for the perturbations have been localized to the ionospheric E-region (neutral wind stream instability, Lyons and Walterscheid, 1985), the high altitude ionosphere (current sheet instability,

Hallinan, 1976) and the plasma sheet in the magnetosphere (Kelvin-Helmholtz instability, Rajaram et al., 1986). A unified approach to some of these perturbations (omega bands and WTS) has been suggested by Rostoker and Samson (1984).

The event reported here is a well defined, eastward travelling loop in a weak auroral arc. This structure is reminiscent of an omega band, since it is shaped like the Greek letter  $\Omega$  and drifts eastward as omega bands do. However, omega bands appear at the edge of the diffuse aurora, whilst the observed structure was on a discrete arc. These properties lead us to classify it as an auroral fold, following the definition of Davis and Hallinan (1976).

The present event is similar to one of the cases modelled by Walterscheid et al. (1985) and Lyons and Walterscheid (1985). They modelled the disturbance of the E- and F-region neutral wind as a result of a symmetric stable auroral arc and a diffuse aurora. For the diffuse auroral case they suggest that a shear instability in the E-region neutral wind could be responsible for omega bands on the poleward border of the postmidnight diffuse aurora. For the discrete arc situation the neutral wind shear is not sufficient to drive auroral waves along discrete arcs.

Auroral spirals (Davis and Hallinan, 1976) are vortex configurations in the aurora. The distinguishing feature of this type of perturbation is the clockwise rotation viewed antiparallel to  $\vec{B}$ . The spiral diameter is in the range 20-600 km. During the initial

stage of a spiral development it is called a fold by Davis and Hallinan (1976) and has a scale of about 20 km. A smaller vortex configuration is the curl (<10 km). The curls are counterclockwise viewed antiparallel to  $\vec{B}$  and are seen as auroral rays when viewed from the side. The spirals and folds are explained by the current sheet instability according to Webster and Hallinan (1973) and Hallinan (1976). The auroral arc constitutes a sheet current. The sheet current generates a transverse magnetic field which causes a shear in the particle flow due to the resultant  $\vec{E} \times \vec{B}$  drift.

Large-scale undulations of the edge of the diffuse aurora have been reported both on the equatorward edge of the oval in the evening sector (Lui et al., 1982) and on the poleward edge of the morningside oval as omega bands and torches (Akasofu and Kimball, 1964). Both have been explained by a shear in the plasma flow (Kelley, 1986; Rajaram et al., 1986). The poleward edge of the oval marks a transition zone from a northward electric field on the poleward side to a southward electric field on the equatorward side (Mozer and Lucht, 1974). Rajaram et al. (1986) propose that the shear zone maps out to the interface between the central plasma sheet and the low latitude boundary layer. The undulations are caused by a Kelvin-Helmholtz instability in that velocity shear zone. The importance of the Kelvin-Helmholtz instability in another velocity shear zone, the magnetopause boundary, has long been studied, and is recently simulated by Miura (1987).

The objective of this study is to use the available data set during the passage of an eastward travelling auroral fold in northern Scandinavia to find evidence for where the cause of the perturbation is localized.

The data consist of incoherent scatter measurements by EISCAT, all-sky camera images, magnetograms, F-region neutral wind observations and data from a HILAT satellite pass.

#### GEOPHYSICAL ACTIVITY

All-sky photographs from Kiruna in northern Sweden, geographic coordinates:  $67.84^{\circ}\text{N}$ ,  $20.41^{\circ}\text{E}$ , L-value; 5.35, show that a diffuse auroral arc appeared approximately above the EISCAT radar station in Tromsö, Norway at about 22 UT on April 8, 1986. The Tromsö radar site is located 200 km north of Kiruna approximately in the magnetic meridian plane through Kiruna. The arc then moved south, a distance of about 70 km, and became more discrete and intense at 2248 UT. Between 2248 UT and 2256 UT the arc did not move significantly in latitude, but developed small distortions together with intensity variations. The arc was then south of the Tromsö magnetic field line. At 2256 UT a stronger distortion of the arc appeared towards the horizon west of Kiruna, which then propagated eastwards as a large fold in the pre-existing arc, crossing the Kiruna magnetic meridian at 2300 UT. After the passage of the fold the auroral luminosity became diffuse and patchy.

In figure 1, upper panel, we display with five frames the arc development. The Tromsö magnetic field line at 110 km height has been marked with a white dot. The Tromsö radar beam, directed along the Tromsö field, sampled the arc when it was diffuse (a)

and during the passage of the fold (c), (d) and (e). When the fold passed the radar beam at 2300 UT (d) it had an eastward speed of  $280 \text{ ms}^{-1}$  as determined from the all-sky images. The east-west extent of the hole is 37 km at 110 km altitude.

A HILAT satellite pass occurred between 2220 UT and 2229 UT, 900 km to the west of Kiruna (1.3 hrs earlier in local time) (figure 2, lower panel). Data were transferred from the Tromsö telemetry station to Kiruna by a dial-up modem. A computer printout of that pass is shown in figure 2. The Kiruna all-sky camera displays a stable diffuse arc at that time, and the Leirvogur magnetogram, figure 3a, (2.7 hrs to the west of Kiruna) shows a stable magnetic situation. We assume therefore that no substorm activity had started at an earlier local time. The HILAT satellite crossed the arc at 800 km altitude. The ion drift meter indicated a westward flow when crossing the oval. The westward ion drift peaks poleward of the particle signature of the arc. The maximum in the westward ion drift corresponds to a northward electric field of  $100 \text{ mVm}^{-1}$ ; assuming an  $E \times B$  drift. When the highest energy flux is measured the ion drift is reduced to almost zero, indicating a reduced electric field within the arc (Vondrak, 1981). The drop in the low energy flux at 2226 UT marks the equatorward edge of the auroral oval.

It is our belief that the arc intensification and the development of folds occurred as a result of an auroral oval activation on the duskside of the magnetic midnight meridian (Shepherd et al., 1978). Local magnetic midnight in Kiruna is at 2125 UT.

The Iceland

magnetogram(figure 3a) shows that close to the midnight meridian the more active period started as early as 2235 UT. The subsequent eastward spreading of auroral activity reached the Kiruna meridian at 2248 UT. It is unclear if the activation should be called a substorm or not.

The passage of the major fold at 2300 UT occurred above Tromsö (figure 1c). Any significant current system belonging to the eastward drifting fold should be seen in the Tromsö magnetogram. Figure 3b shows that the D- and Z-component in Tromsö run through a negative/positive sequence when the fold passes overhead. The D-component lags the Z-component by a few s (difficult to see in the published figure). The peak-to-peak amplitude in Z is 28 nT. The strong decrease in the H-component, reaching 290 nT later, we consider to be due to a general increase in the westward electrojet and not belonging to the fold current system.

The thermospheric neutral wind measured at about 240 km altitude using the [OI] emission at 630.0 nm (Rees et al., 1983) is shown in figure 4. The meridional neutral wind is slightly southward,  $50 \text{ ms}^{-1}$ , during the period except for one significant measurement at 2238 UT. The zonal neutral wind is close to zero but with a small westward tendency.

The night of April 8 was only moderately disturbed,  $K_p$  reached a value of 2 for the studied period.

## EISCAT OBSERVATIONS

The experimental mode operated by EISCAT during this interval was CP-1-F, which gives ACF measurements between 84 and 169 km altitude with 2.9 km height separation, and between 154 and 734 km with 26.3 km separation. Because the interesting features of this event varied rather rapidly with time, the data were analysed using 20 s averages. Short integration periods usually give poor estimation of plasma parameters from the E-region pulse code part of the experiment, so we shall only discuss measurements of raw electron density for E-region heights. The F-region results, however, are reliable, and we shall especially examine the ion temperature and electric field measurements.

The spike-like increase of E-region electron densities at 2259 UT (figure 5) marks the crossing of the radar beam by the leading edge of the fold. A spike is also observed in F-region densities (figure 6), but is progressively later at higher altitudes, amounting to a delay of the order of 1 minute between altitudes 120 and 350 km (figure 7). Before this, whilst the arc was still to the south of the radar, two maxima in F-region ion temperature were observed at 2250 and 2255 UT, the second of these reaching about 2700 K at most heights (figure 8).

The remote site antennas spend 5 minutes of the 10 minute CP-1 cycle in the F-region, and figure 9 shows the computed horizontal drift vectors at 312 km. Before 22 UT (not shown) the velocities were small (below  $100 \text{ ms}^{-1}$ ), but after 22 UT a gradual increase

in velocity, almost directly east, was observed. This pattern is characteristic of the radar moving under the eastward convection cell in the post-midnight sector, and the variations on this background field are the disturbance effects associated with the deformation of the auroral arc.

#### INTERPRETATION OF OBSERVATIONS

The increased activity may already have started as early as 2235 UT, as seen from magnetograms from Leirvogur, Iceland (figure 3a). At Tromsö the increased activity was seen as two large ion temperature increases at 2250 UT and 2255 UT. The radar beam was north of the discrete arc at these times. The ion drift measurements in the interval 2250 UT to 2255 UT show a positive correlation with the ion temperature (figure 10 and 11), and we interpret the ion temperature increases as Joule heating due to intensified electric fields. Detailed study of the all sky photographs also show that the arc increased in brightness at the times of increased electric field.

In addition to the major fold discussed here, two earlier attempts of fold development were identified from all-sky images (not shown). They looked like eastward drifting interruptions in the arc brightness. The identified folds are marked in figure 10, together with a detailed plot of F-region ion temperature.

Thus the folds in the arc appear to be a result of the electric field intensifications. The first intensification (A in figure

10) was accompanied by one observed fold, and the second (B) by two folds. The increase of ion temperature during the third (major) fold may also be ascribed partly to particle heating associated with the more intense precipitation; this was the only time during the event that the F-region electron temperature showed a significant increase (not illustrated here).

We consider the two electric field enhancements to be of large scale origin and not travelling with the fold structures. The reason for this is that the arc brightness over the all-sky camera field of view responded uniformly to the electric field intensifications.

Of special importance, for the understanding of the perturbation in the arc, we consider the dispersion in energy. Figure 7 is a detailed plot using the highest possible time resolution (10 s). The leading edge of the fold entered the radar beam at 2259 UT (figure 1c). The enhanced E-region precipitation between 2258 UT and 2259 UT belongs to the pre-existing arc which moved northward at the time of fold arrival. With the arrival of the leading edge of the fold the ionization builds up at progressively higher altitudes. This can be explained by the softer precipitation (corresponding to altitudes  $\geq 200$  km) arriving later than the harder precipitation ( $\sim 120$  km altitude) when the leading edge (as seen optically) enters the beam. The ionization peak in the E-region corresponds well in time to the arrival of the edge as seen from all-sky camera. The ionization at 250 km altitude lags

the ionization at 120 km altitude by 30 s. The peak in the upper F-region ionization appears to come in the hole of the fold, as determined from the all-sky images.

In the theory for auroral spirals by Webster and Hallinan (1973) (current-sheet instability), the transverse (to  $\vec{B}$ ) velocity of the precipitating electrons is given by

$$v_T = \frac{v\mu_0 jx}{B} \quad [\text{ms}^{-1}] \quad (1)$$

where  $v$  = velocity of the electron along original  $\vec{B}$  direction

$B$  = earth magnetic field intensity

$j$  = current density

$x$  = the width of the pre-existing arc

$\mu_0$  = permeability for vacuum

In this theory the transverse drift velocity is energy dependent. The difference in arrival time,  $\Delta t$ , for two electrons of different energies, 1 keV (250 km altitude) and 10 keV (120 km altitude) is

$$\Delta t = L \left( \frac{1}{v_1} - \frac{1}{v_{10}} \right) \quad [\text{s}] \quad (2)$$

where  $L$  = some (yet unspecified) distance

$v_T^1$  = transverse velocity of 1 keV electron

$v_T^{10}$  = transverse velocity of 10 keV electron.

According to Hallinan (1976)  $j=8 \cdot 10^{-6} \text{ Am}^{-2}$  for a well-developed spiral. For the other quantities in (1) we use  $B=50000 \text{ nT}$ ;

$\mu_0=4\pi \cdot 10^{-7} \text{ VsA}^{-1} \text{ m}^{-1}$ , and the velocities are calculated ( $v=\sqrt{2 \cdot E(\text{keV})/\text{m}}$ ) to be  $v^{10}=5.9 \cdot 10^7 \text{ ms}^{-1}$ ;  $v^1=1.87 \cdot 10^7 \text{ ms}^{-1}$ .

Thus

$$\Delta t = \frac{L}{x} \cdot 0.19 \quad [\text{s}] \quad (3)$$

To obtain  $\Delta t=30 \text{ s}$  from (3) we need that the electrons would have drifted 157 times the width of the arc. In our case we estimate the arc width to be 1 km. Since the size of the hole was 37 km we do not think the current sheet instability can explain the observed fold. In addition no rotation could be identified which is a characteristic feature for spirals and explained by the current sheet instability.

We did not measure the E-region neutral wind close to the arc which is necessary to test the theory by Lyons and Walterscheid (1985). However they point out that the neutral wind shear instability will not be sufficient for stable discrete arcs. Also our F-region neutral wind measurements give no indication of any enhanced neutral wind at the time of the fold. At this stage we bring up

the matter of spatial separation between the various measurements used here. The HILAT satellite passed the arc at 2225 UT (1.3 hrs earlier in local time) and measured a westward plasma flow of almost  $2000 \text{ ms}^{-1}$ . At the same time the EISCAT radar indicates a  $500 \text{ ms}^{-1}$  ion drift mainly eastward and increasing up to  $2000 \text{ ms}^{-1}$  at 23 UT. The F-region meridional neutral wind is measured approximately 200 km north of Tromsö and has a southward direction. Instead of an eastward neutral flow the zonal neutral wind speed is clearly directed towards the west (as seen in mirror position: east and north east). The disagreement between the HILAT and EISCAT measurements can be explained by the HILAT pass having occurred in the westward convection cell whilst the EISCAT measurements took place in the eastward convection cell. The opposite direction of the zonal speed for the ions and the neutrals may have some physical implication for the perturbation of the arc. We also note that the meridional neutral wind is blocked at 2238 UT coinciding in time both with the onset of the electric field intensification (figure 8) and the onset of magnetic disturbance at Iceland (figure 3a). These type of observations are the subject of a separate publication and will not be discussed further here.

The difference in bounce-time, from the equatorial plane to the ionosphere, for a 1 keV and a 10 keV electron is about 1.5 s, using formulas given by Roederer (1970). The combined gradient-curvature drift is energy dependent, and eastwards for electrons. The drift speed for a 1 keV electron is 0.05 deg. per min, and for a 10 keV electron 0.5 deg. per min. (Roederer, 1970). To obtain  $\Delta t = 30 \text{ s}$

we need a drift distance of 0.03 deg. in longitude, which amounts to 1.3 km in the ionosphere. However the energy dependent azimuthal drift cannot explain the observed dispersion in energy since the width of the radar beam at F-region altitudes has about the same dimensions (~ 3 km).

Another way of understanding the delayed arrival of the soft precipitation is by ascribing the soft population to a magnetospheric instability responsible for the perturbation of the arc. Akasofu (1971) suggested that the omega band is a manifestation of large-scale ripples on the surface of the expanding plasma sheet. Rostoker and Samson (1984) and Rajaram et al. (1986) developed this idea further by suggesting that the perturbation of auroral forms maps out to a region where the Kelvin-Helmholtz instability (KHI) is developed. The radar beam probed the ionosphere poleward of the arc until the arc moved northward at 2258 UT (figure 7) and the leading edge of the fold reached the beam at 2259 UT. The soft precipitation exclusively belonged to the hole in the fold and did not occur prior to or after the passage of the hole. We propose that the soft precipitation originates from the process creating the deformed arc. If KHI is the responsible process it should be able to accelerate electrons up to several hundreds of eV. Thompson (1983) proposed that the KHI can develop field-aligned potential drops of several keV.

Figure 12 is a suggested scheme for the current system responsible for the observed magnetic variations at Tromsø around 2300 UT

(figure 3b). The current system is similar to the one proposed by Gustafsson et al. (1981) for Ps6 pulsations. Maximum southward current occurs at the time of the negative peak in the magnetic D component, and is slightly later than the intense precipitation. Variations in the Z component follow the pattern expected for a southward current drifting eastward. Upward current is carried by the large fluxes of precipitating electrons at the leading edge of the fold, but the identification of the location of the downward current closing the circuit is difficult to deduce from the observations.

#### SUMMARY AND CONCLUSION

We have observed an eastward drifting fold in a pre-existing auroral arc. In the ionosphere the arrival of the fold was preceded by two major electric field intensifications. The hole in the fold is characterized by soft (a few hundred eV) electrons precipitation. In comparison to the two major ion temperature increases the ion temperature variation associated with the hole in the fold was considerably smaller, suggesting that the hole is not characterized by any strong ionospheric electric field signature.

We interpret the deformation in the auroral arc as resulting from strong large-scale ionospheric electric field intensifications ( $100 \text{ mVm}^{-1}$  at 312 km altitude). We suggest that the cause of the fold is to be found in the magnetosphere, probably in a velocity shear zone where the Kelvin-Helmholtz instability can be activated. The ionospheric electric field intensifications are interpreted as the ionospheric signature of enhanced plasma flow

velocity in the magnetosphere. We suggest the Kelvin-Helmholtz instability should be investigated further to find out if it can produce the observed soft precipitation in the hole of the fold.

## Acknowledgments

The EISCAT Scientific Association is supported by the Centre National de la Recherche Scientifique of France, Suomen Akatemia of Finland, Max-Planck Gesellschaft of West Germany, Norges Almenvitenskaplige Forskningsråd of Norway, Naturvetenskapliga Forskningsrådet of Sweden and the Science and Engineering Research Council of the United Kingdom.

The HILAT data was received as a part of a collaboration between the Swedish Institute of Space Physics in Kiruna and AFGL in Boston covered by the USAF Grant No. AFOSR-84-0084.

We are thankful to the observatories in Tromsö, Norway and Leirvogur, Iceland for providing magnetograms, and to Dr. David Rees, University College London for providing analysed neutral wind data.

REFERENCES

- Akasofu S.-I. and Kimball D.S. 1964 J. Atmos. Terr. Phys. 26, 205.
- Akasofu S.-I., Hones E.W., Jr., Montgomery M.D., Bame S.J. and Singer S. 1971 J. Geophys. Res. 76, 5985.
- Akasofu S.-I., Meng C.-I. 1966 J. Atmos. Terr. Phys. 28, 489.  
and Kimball D.S.
- Davis T.N. and Hallinan T.J. 1976 J. Geophys. Res. 81, 3953.
- Gustafsson G., Baumjohann W. and Iversen I. 1981 J. Geophys. 49, 138.
- Hallinan T.J. and Davis T.N. 1970 Planet. Space Sci. 18, 1735.
- Hallinan T.J. 1976 J. Geophys. Res. 81, 3959.
- Hasegawa A. 1970 Phys. Rev. Lett. 24, 1162.
- Kelley M.C. 1986 J. Geophys. Res., 91, 3225.
- Lui A.T.Y., Meng C.-I. and Ismail S. 1982 J. Geophys. Res., 87, 2385.

- Lyons L.R. and 1985 J. Geophys. Res. 90, 12321.
- Walterscheid R.L.
- Miura A. 1987 J. Geophys. Res. 92, 3195.
- Mozer F.S. and Lucht P. 1974 J. Geophys. Res. 79, 1001.
- Oguti T. 1974 J. Geophys. Res. 79, 3861.
- Rajaram G., Rostoker G. 1986 Planet Space Sci., 34, 319.  
and Samson J.C.
- Rees D., Charleton P.J., 1983 Proceedings ESA Symposium on  
Lloyd N., Steen Å. and European rocket & Balloon  
Witt G. programmes, Interlachen,ESA  
SP-183, p. 53.
- Roederer J.G. 1970 Dynamics of Geomagnetically  
Trapped Radiation, Springer-  
Verlag, New York.
- Rostoker G. and 1984 Geophys. Res. Lett. 11, 271.  
Samson J.C.
- Shepherd G.G., Anger C.D. 1987 Geophys. Res. Lett., 14, 395.
- Murphree J.S. and
- Vallance Jones A.
- Steen Å. and 1981 Planet. Space Sci. 29, 1011.  
Gustafsson G.

- Steen A. and Rees D. 1983 Proceedings of the 11th annual  
meeting of upper atmosphere  
studies by optical methods,  
Max-Planck-Institut für  
Aeronomie, Katlenburg-Lindau,  
Editors G. Lange-Hesse and H.  
Lauche, p. 63.
- Thompson W.B. 1983 J. Geophys. Res. 88, 4805.
- Vondrak R.R. 1981 Physics of Auroral Arc Formation, Geophys. Monogr. Ser.,  
vol. 25, edited by S.-I.  
Akasofu and J.R. Kan, p. 185,  
AGU Washington, D.C.
- Walterscheid R.L., Lyons 1985 J. Geophys. Res. 90, 12235.  
L.R. and Taylor K.E.
- Webster H.F. and 1973 Radio Science, 8, 475.  
Hallinan T.J.

## FIGURE CAPTIONS

Figure 1. Upper panel: All-sky photographs from Kiruna showing the development of the large fold in the pre-existing auroral arc on April 8, 1986. The time display (year, dayno, hr, min, sec) is in the geomagnetic east direction. The white dot indicates that the Tromsö field line at 110 km altitude, and is in the geomagnetic north direction. The five sequences show

- a) Original weak diffuse arc. The EISCAT radar measures within the arc. HILAT passes the arc to the west of Kiruna.
- b) The arc intensifies and moves south. The EISCAT field-aligned measurements are made on the poleward side of the arc.
- c) The leading edge of the fold crosses the radar. The fold propagates eastwards at a velocity of 280  $\text{ms}^{-1}$ .
- d) The hole in the fold crosses the radar beam.
- e) The fold is far to the east. The arc becomes diffuse and is probed by the radar.

Lower panel: Altitude profiles of electron density (20 s averages) measured by EISCAT close in time to the frames shown in the upper panel. When the leading edge crossed the beam (c) the ionization peaked at 150 km.

The hole is characterized by a broad F-region ionization. In the diffuse arc (e) after the passage of the fold the ionization peaks at about 125 km altitude similar to the diffuse pre-existing arc in (a).

Figure 2. HILAT data for April 8, 1986, 2220 UT to 2229 UT. The HILAT satellite crossed the arc 900 km west of Kiruna (K in lower panel). The lower panel shows the HILAT pass projected down to 100 km altitude in geographic coordinates. Assuming the quiet diffuse arc was the same at an earlier local time it can be seen as a two orders of magnitude increase in the high energy flux. The location of the arc at 2225 UT has been sketched in the lower panel.

Figure 3a. Magnetogram from Leirvogur, Iceland

Geographic coordinates:  $64.2^{\circ}\text{N}$ ,  $21.7^{\circ}\text{W}$ , L-value: 6.0.  
The disturbance period starts at 2235 UT.

Figure 3b. Magnetogram from Tromsö, Norway

Geographic coordinates:  $69.7^{\circ}\text{N}$ ,  $18.9^{\circ}\text{E}$ , L-value: 6.2.  
The signature of the major fold at 2300 UT is a negative/positive sequence in the D and Z-component.

Figure 4. F-region neutral wind data for April 8, 1986, 21-24 UT. Four directions are shown: geomagnetic north, east, northwest and northeast. Positive wind direction is south, west, southeast and southwest respectively.

Figure 5. Time series of raw electron densities for selected altitudes in the E-region for 1 hour before and after the passage of the fold. The values are averages over 20 s.

Figure 6. As figure 5, but for several F-region gates. The electron density spike associated with the fold is clearly seen at all altitudes, but is progressively later with increasing height.

Figure 7. Raw electron density for the E- and F-region using highest possible time resolution (10 s). The leading edge of the fold enters the radar beam already at 2258:00 UT.

Figure 8. As figure 6, but for ion temperature. Two major maxima can be seen during the ten minutes before the fold reached the radar.

Figure 9. Horizontal ion drift velocity at 312 km, determined from tristatic measurements. The gaps are when the remote antennas were receiving from the E-region, otherwise the values are 20 s averages.

Figure 10. Detailed ion temperature variations at 312 km altitude during the period of auroral activity. The main features of the changes in the aurora are indicated.

Figure 11. Detailed ion drift velocity components at 312 km around the time of the passage of the fold. The first two maxima in ion temperature in figure 10 correspond to large velocities (at 2250 UT and 2255 UT), indicative of Joule heating.

Figure 12. A model for the current system belonging to the eastward drifting auroral fold.

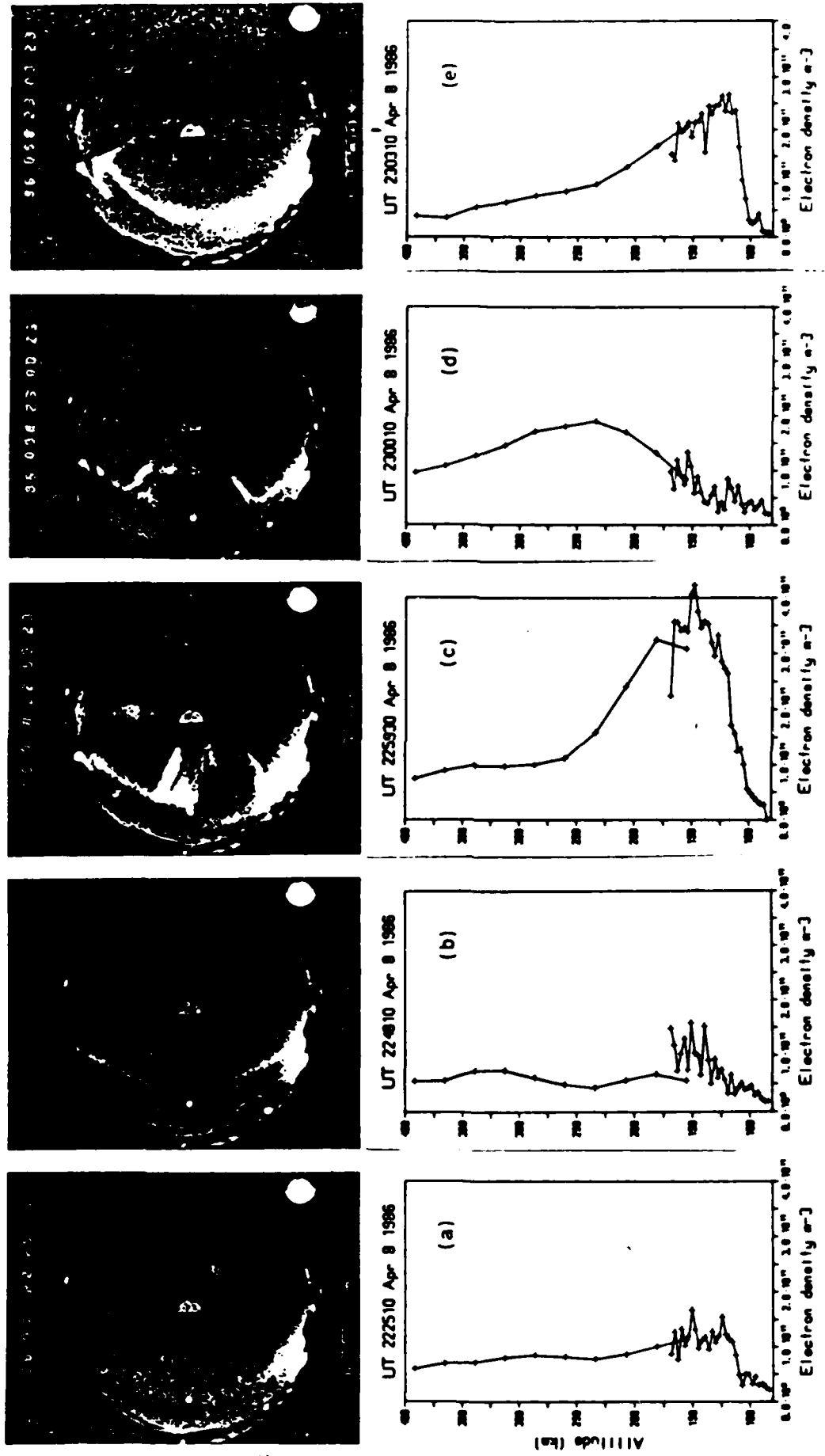
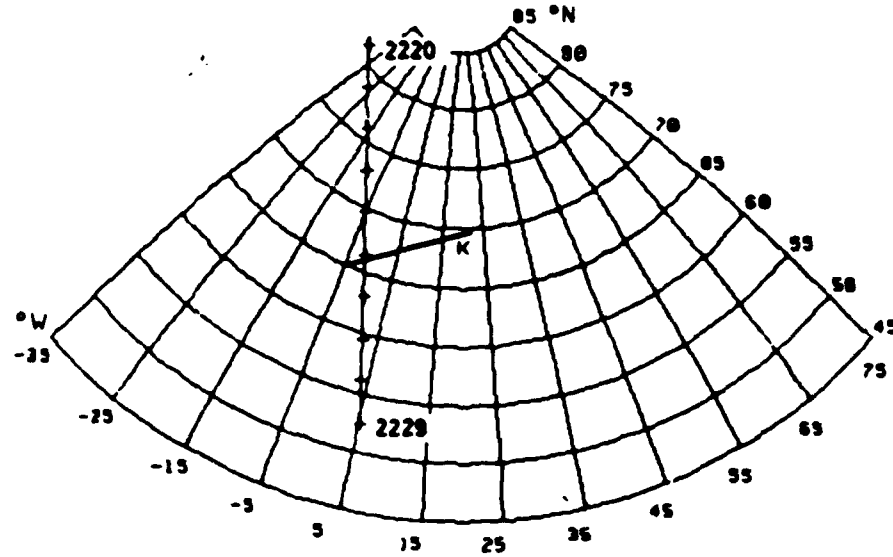
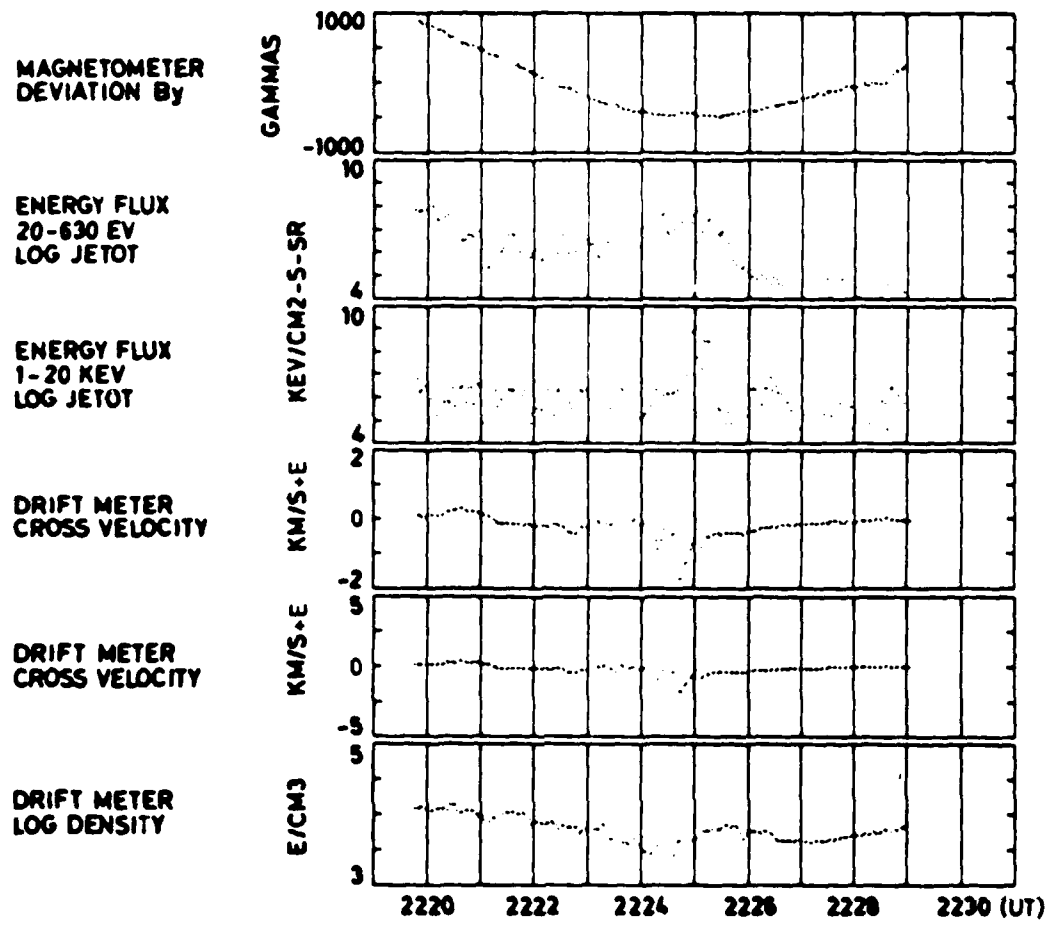


Figure 1



**Figure 2**

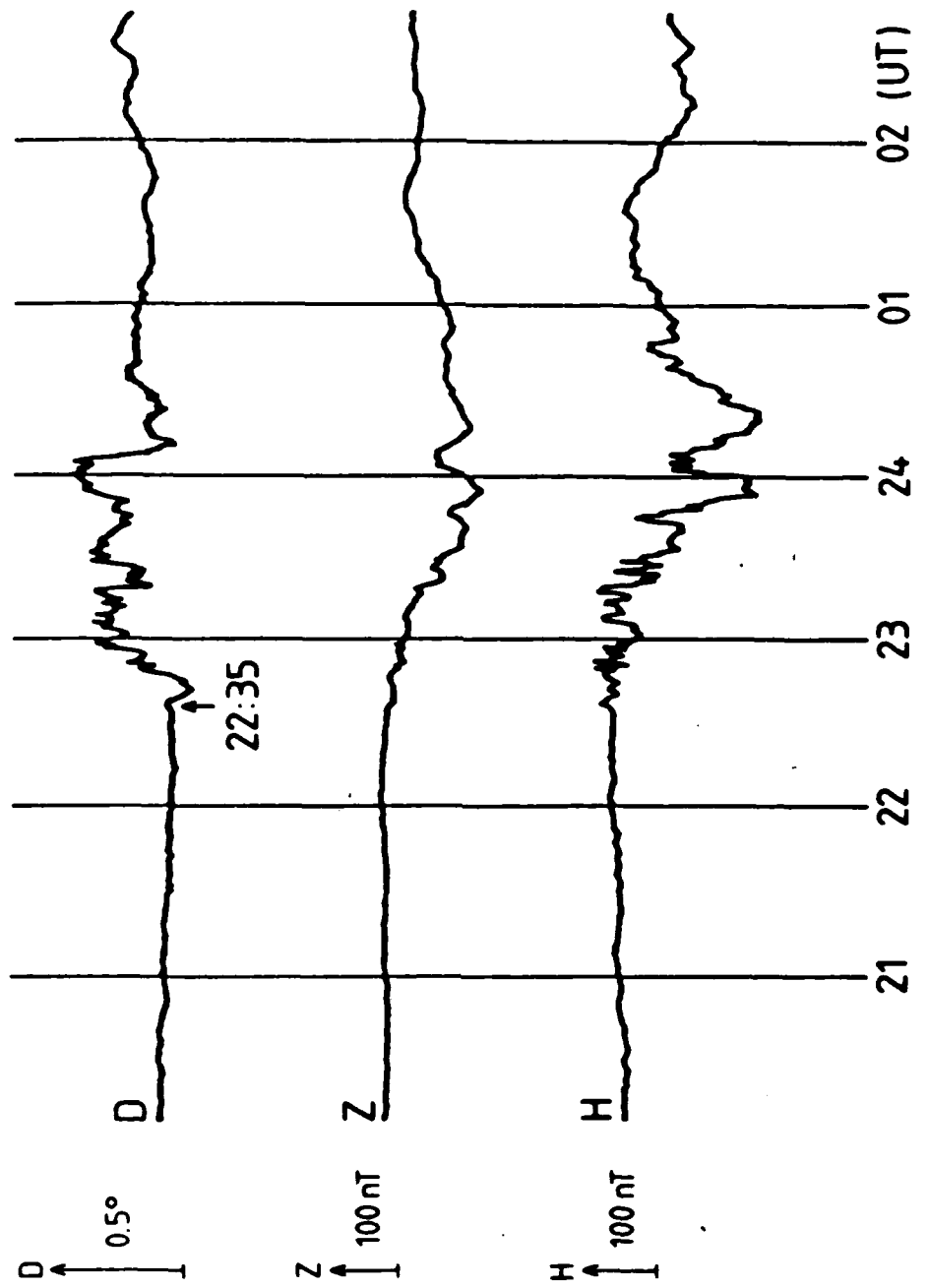


Figure 3 •

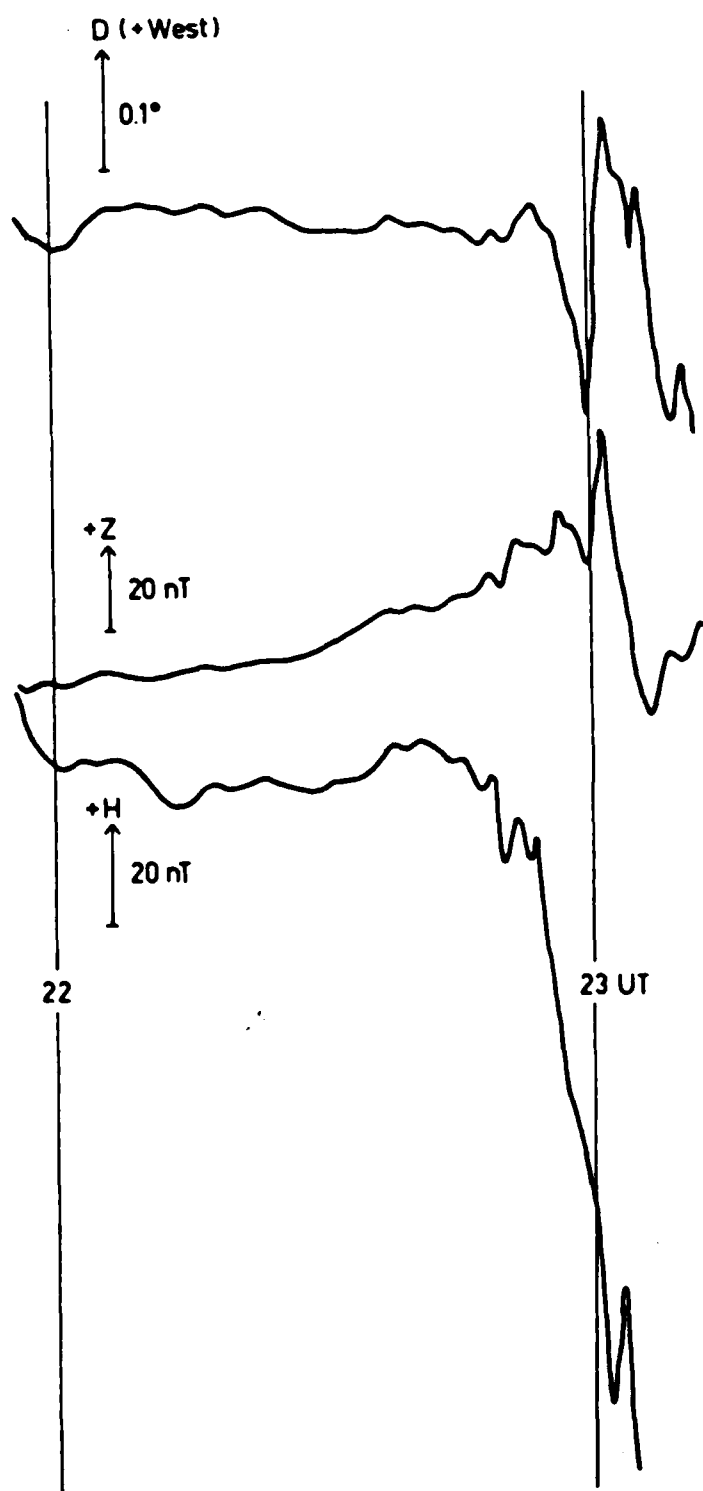


Figure 3 b

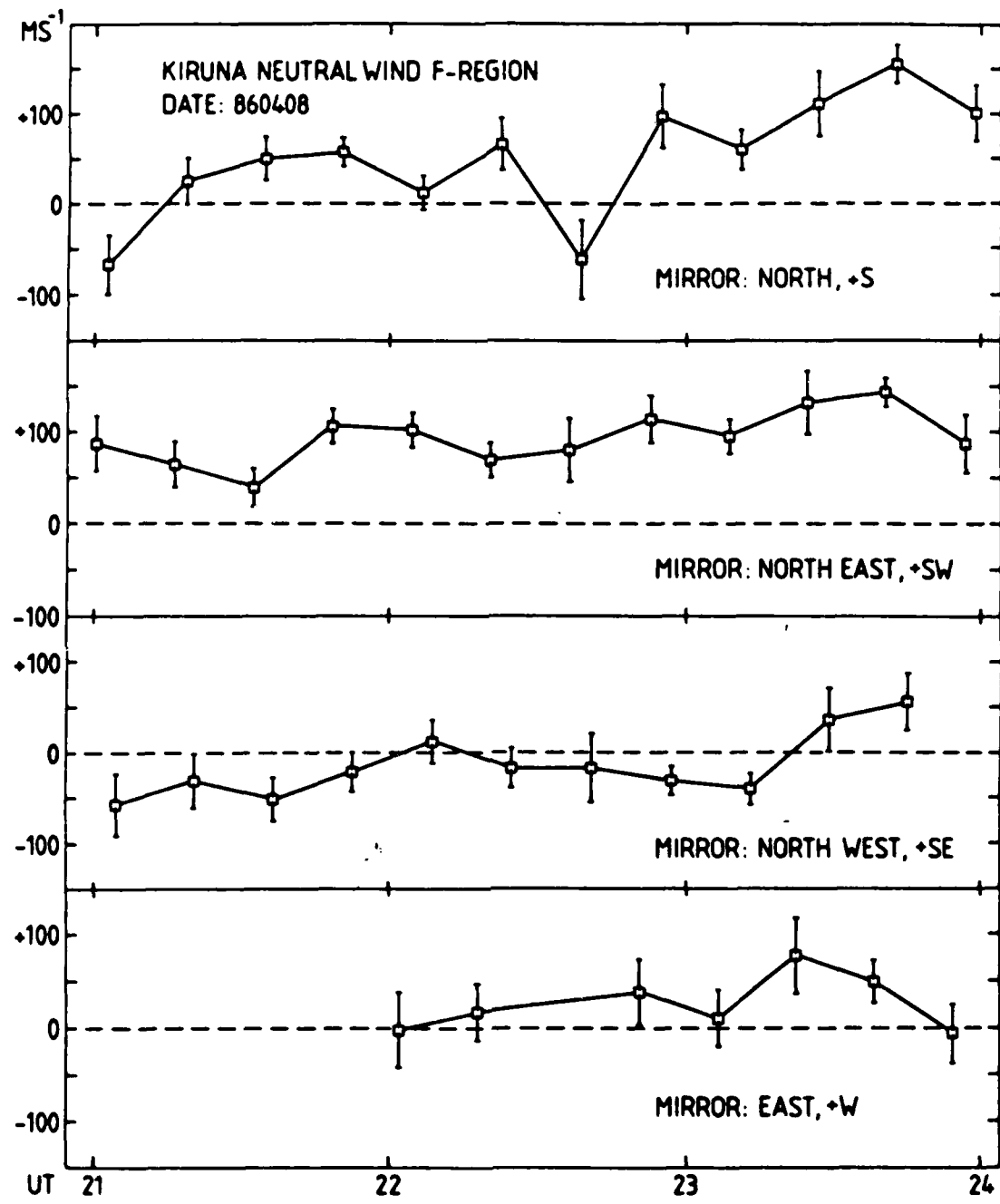
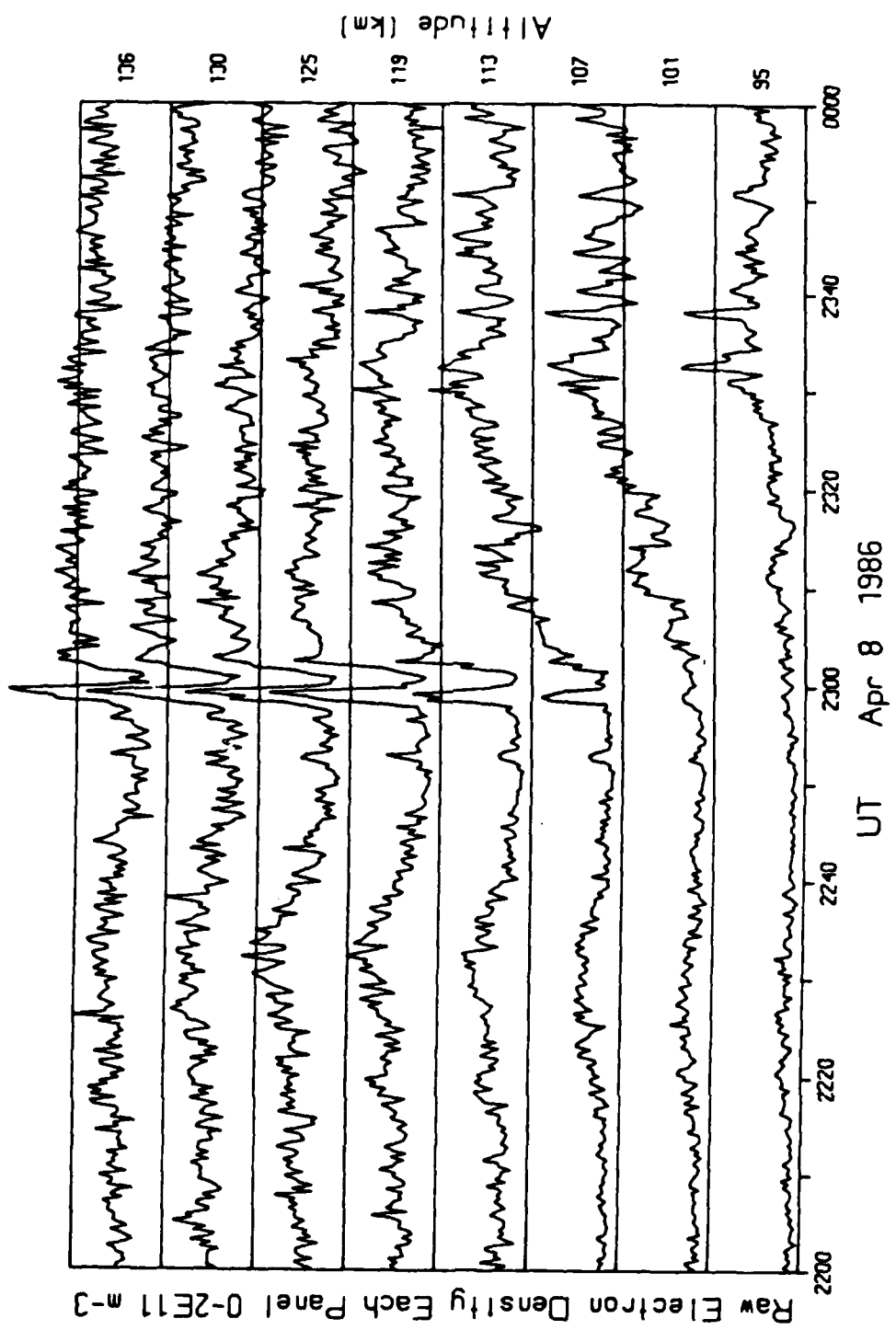


Figure 4

Figure 5



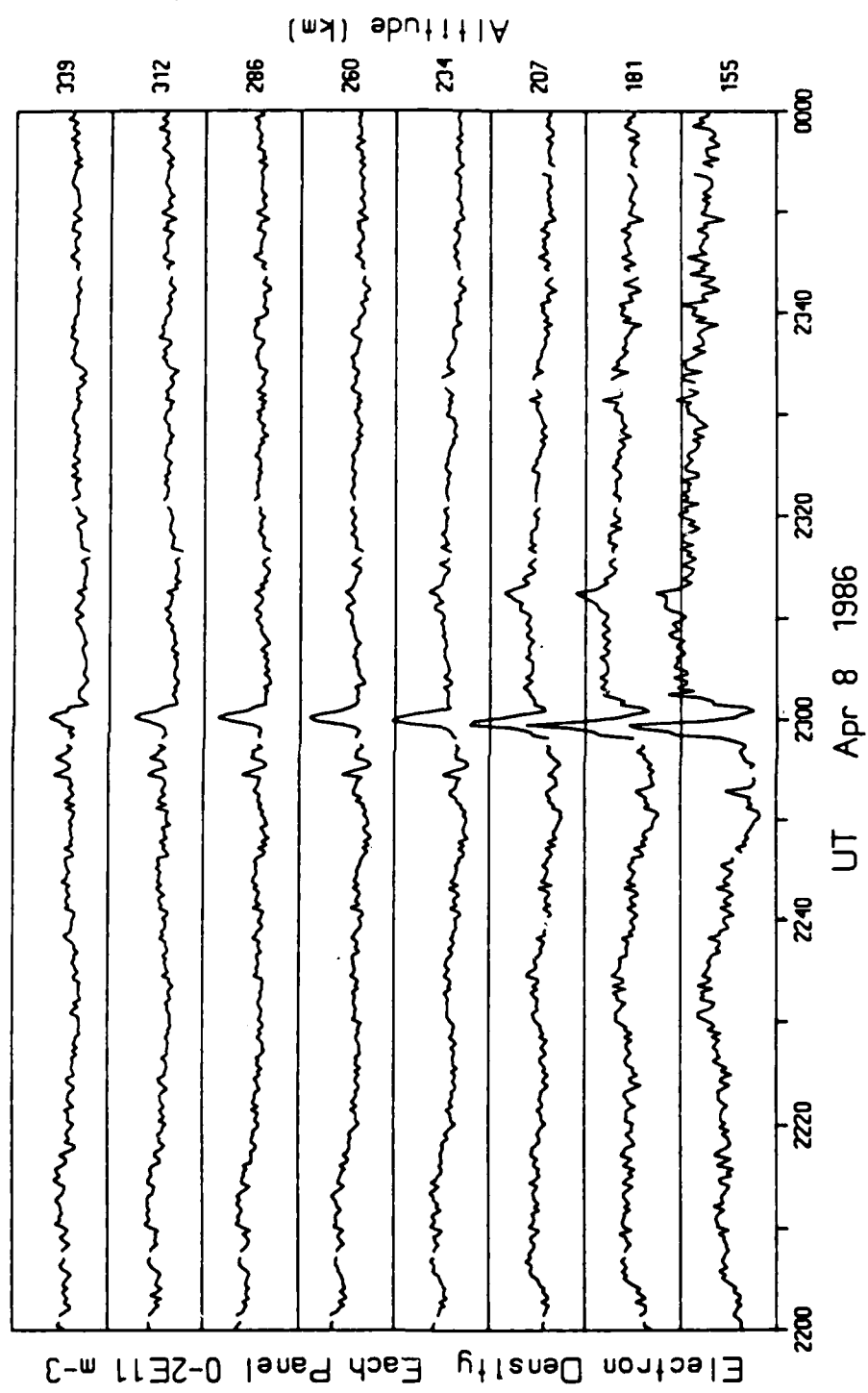


Figure 6

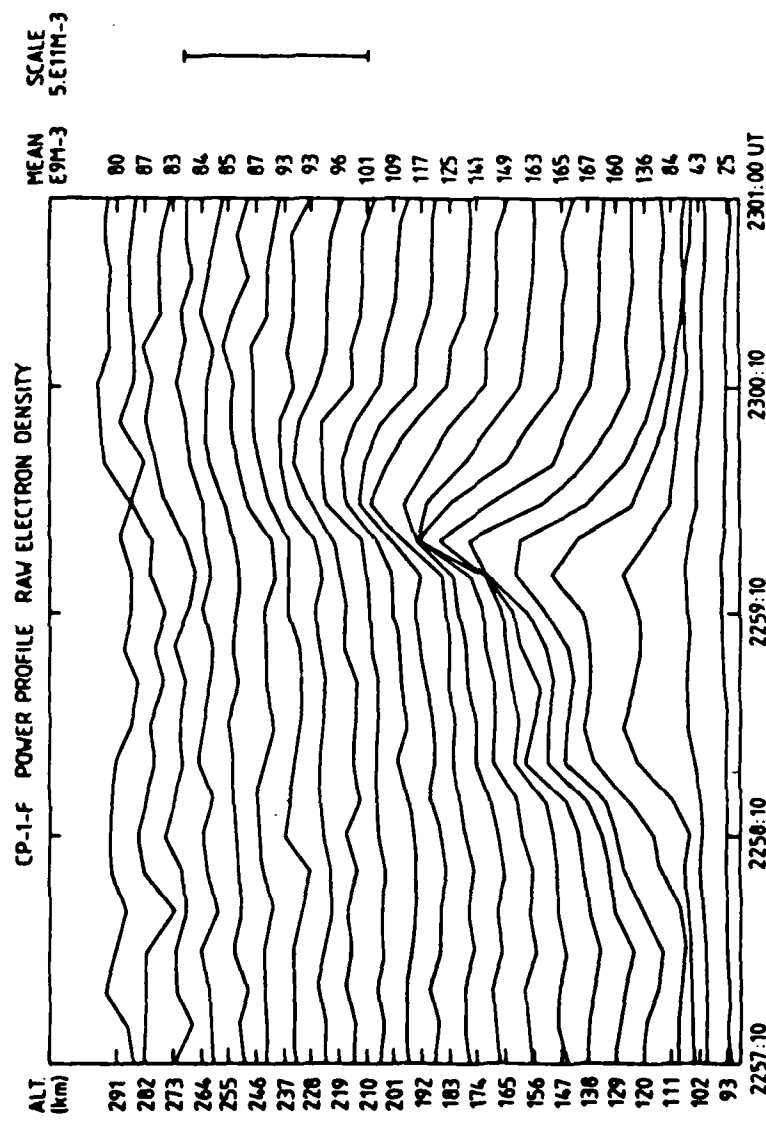


Figure 7

Figure 8

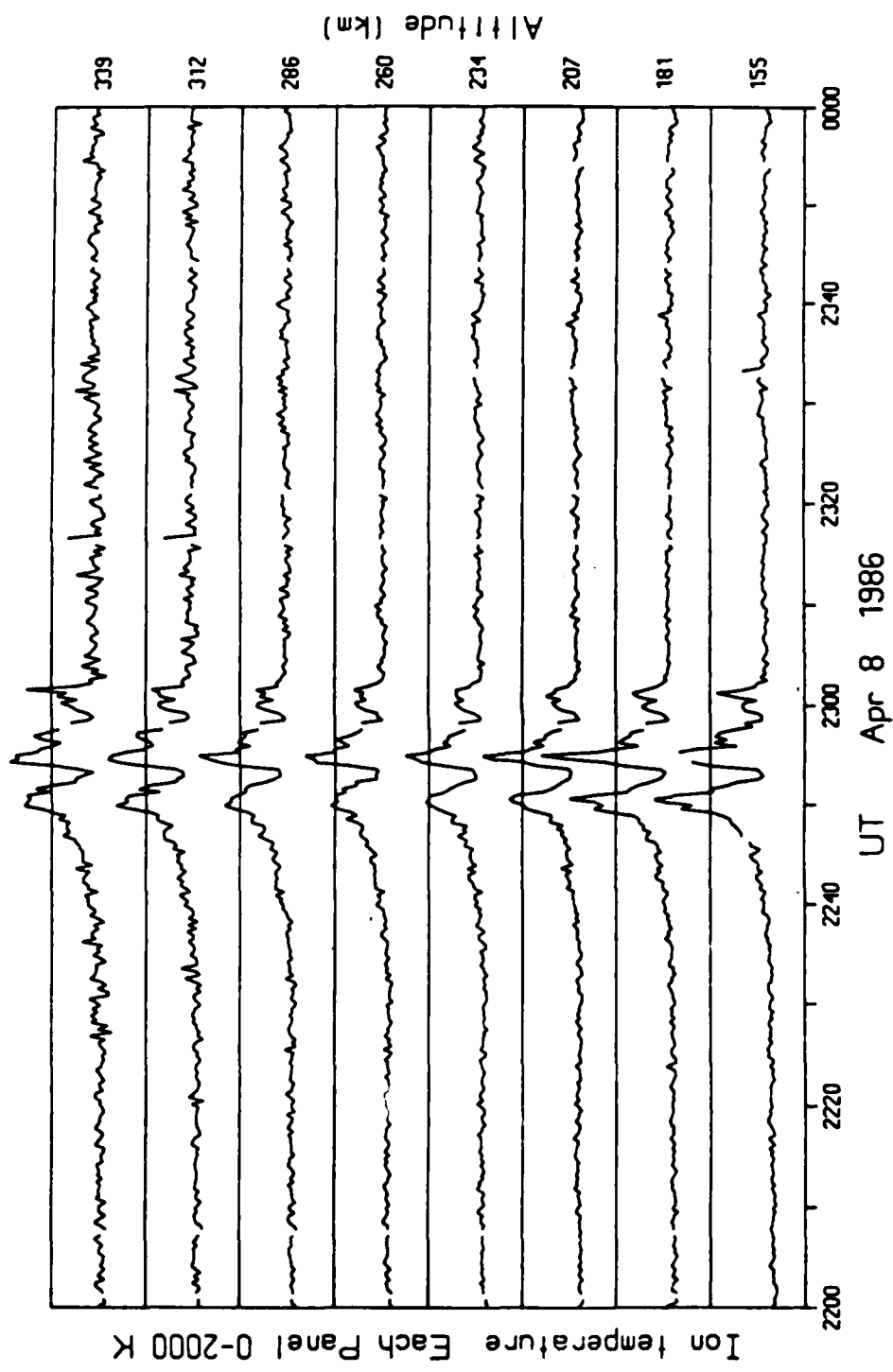
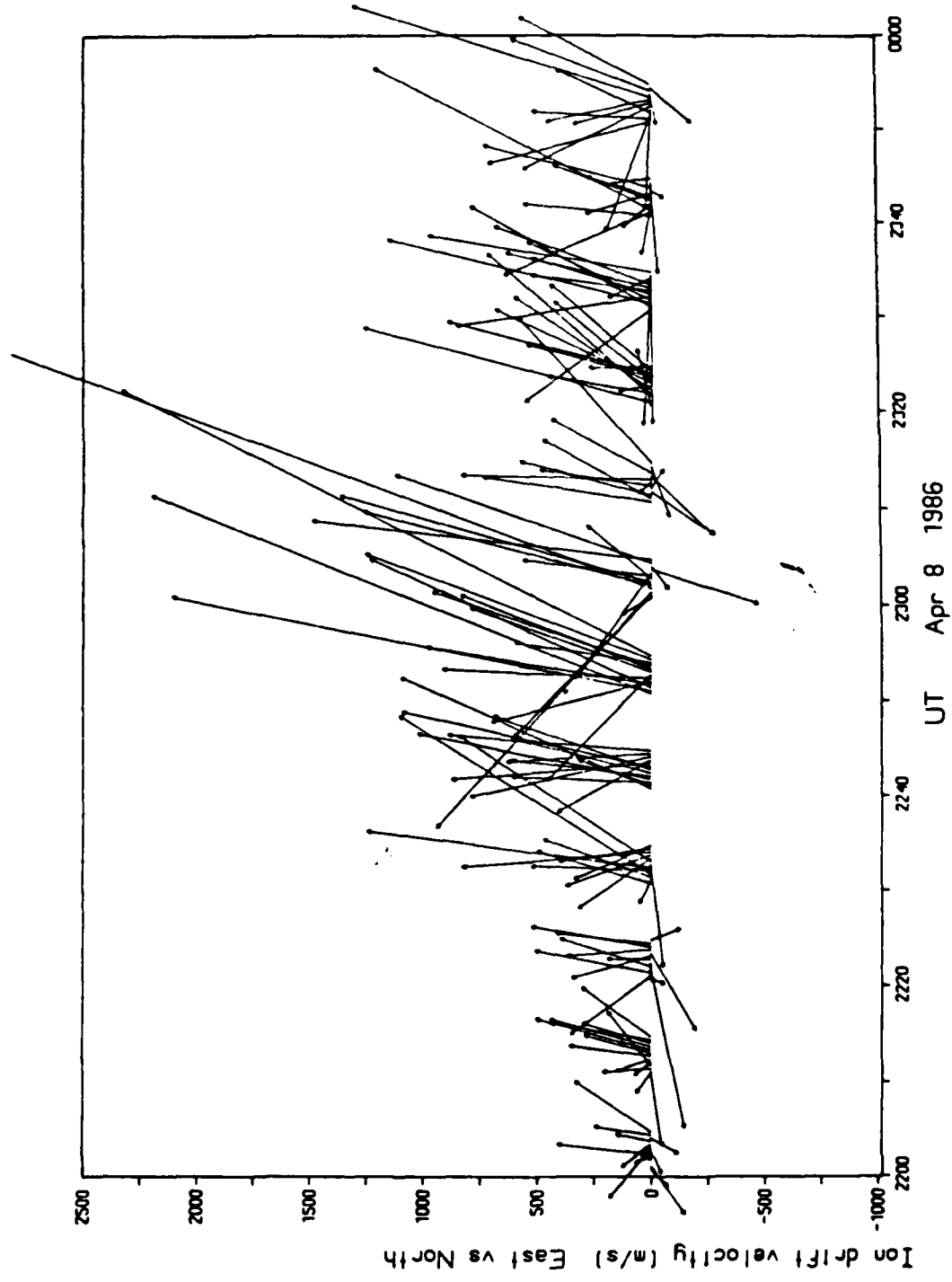


Figure 9



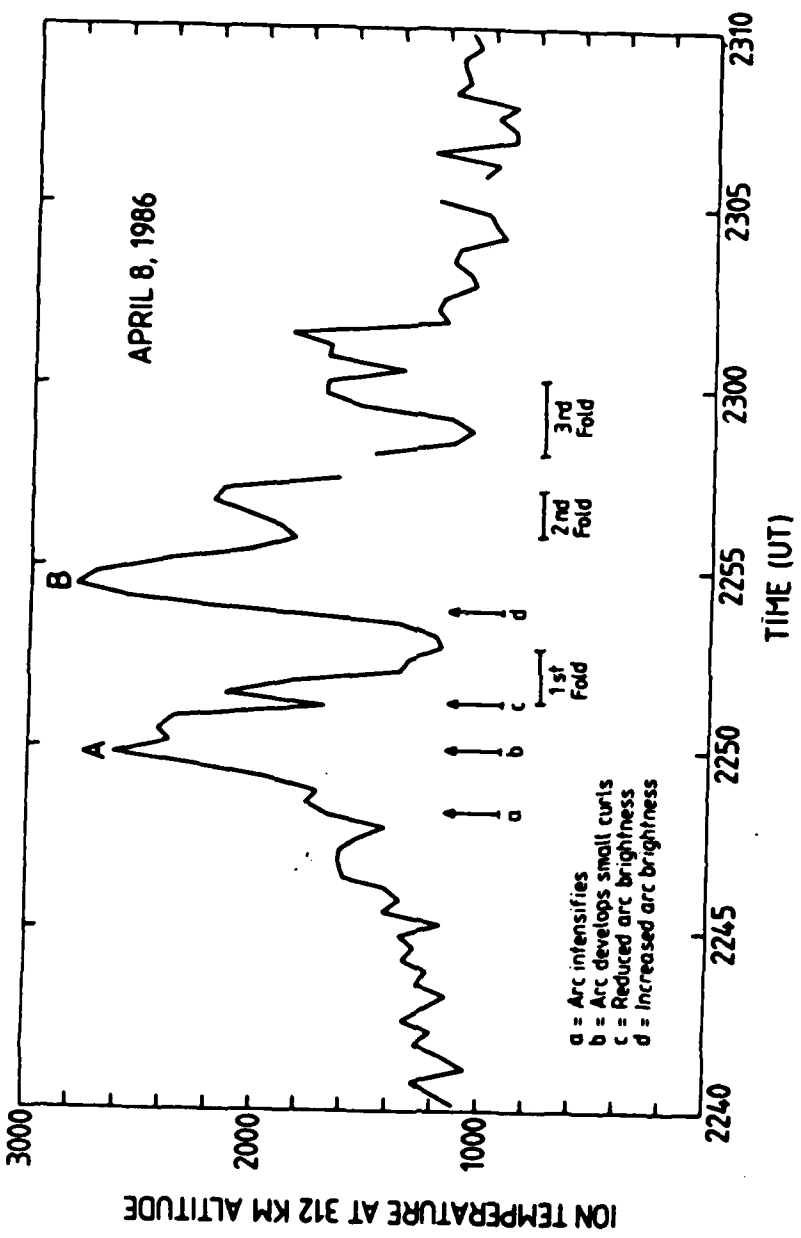


Figure 10

Figure 11

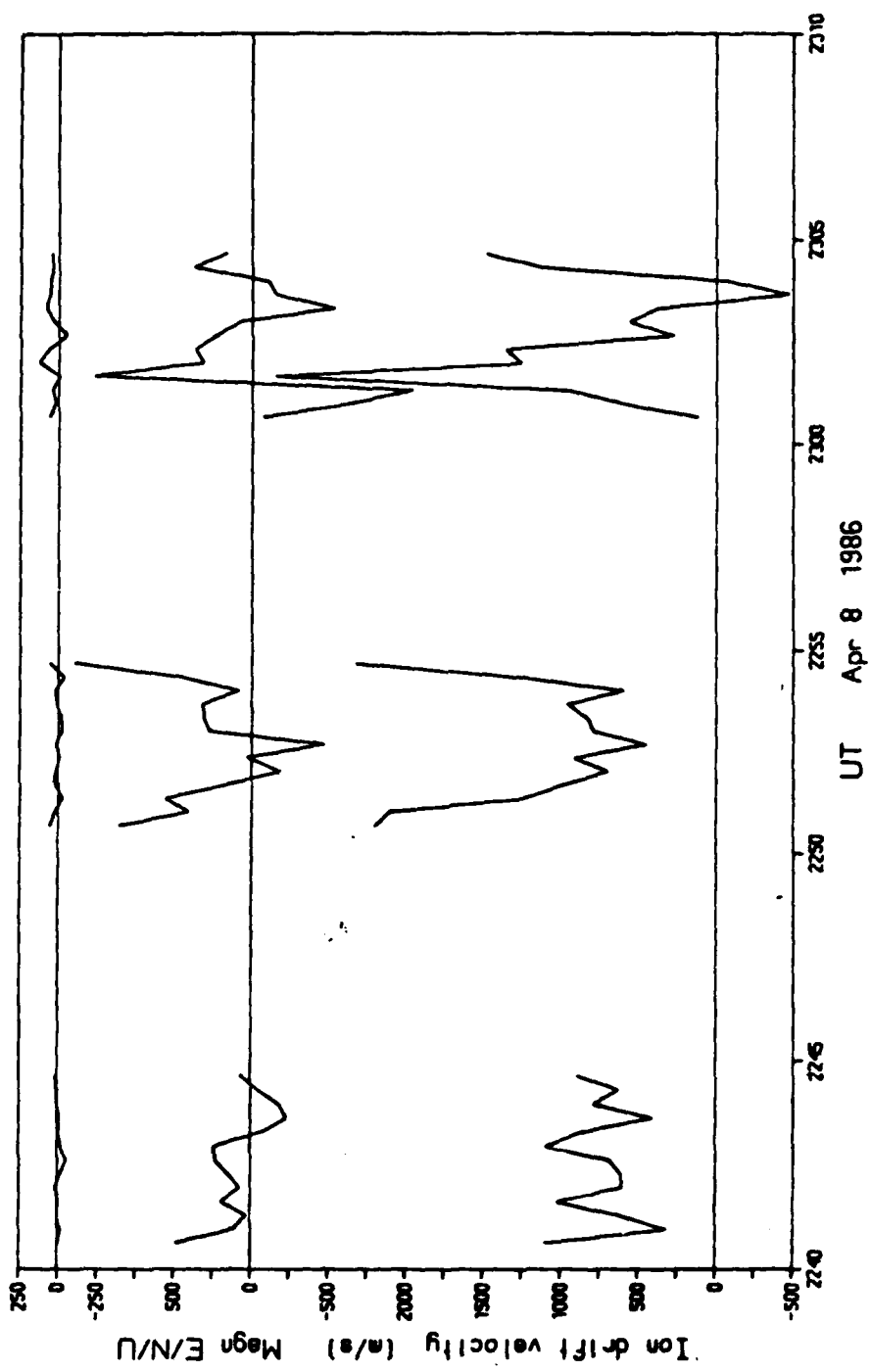
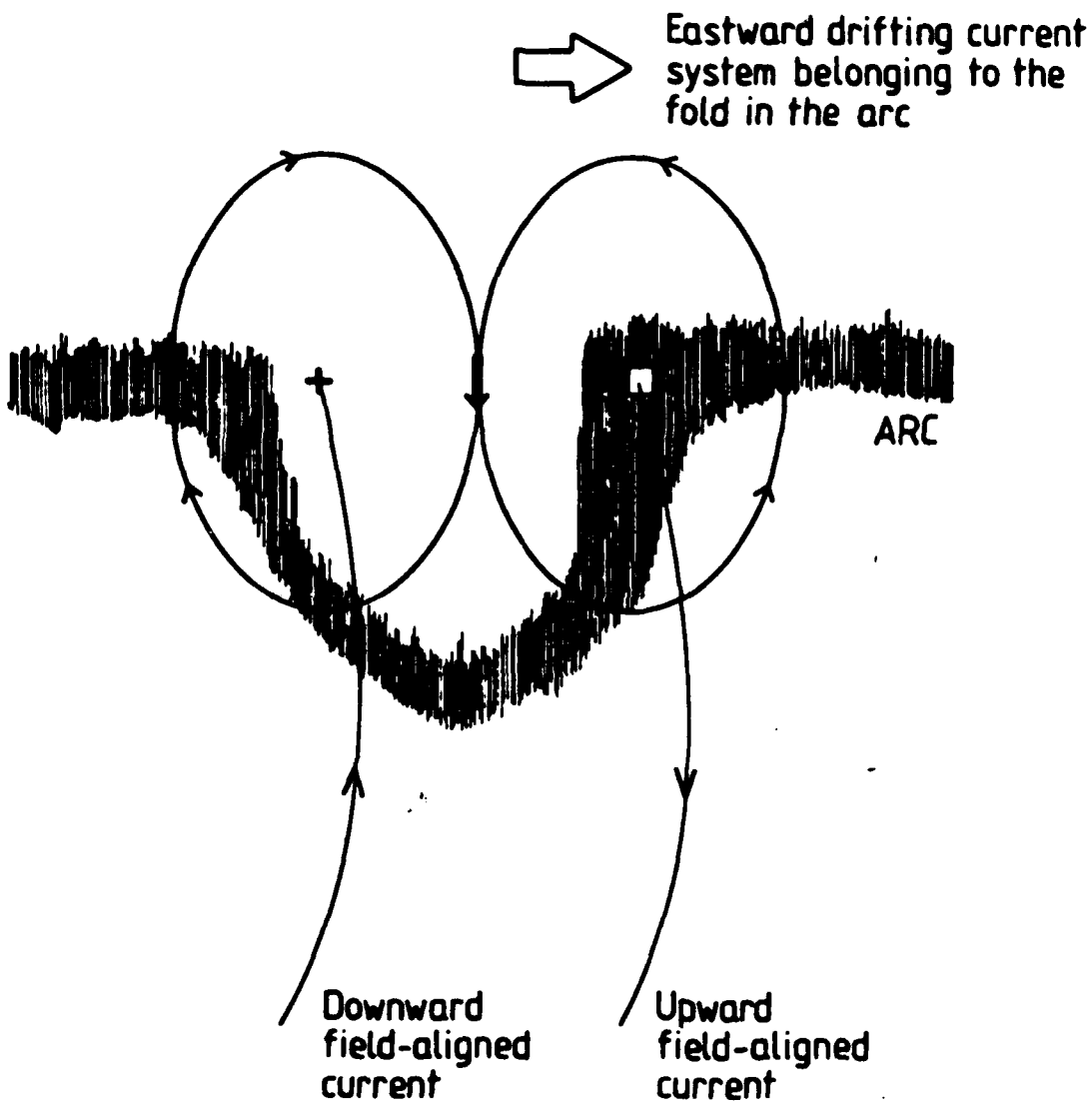
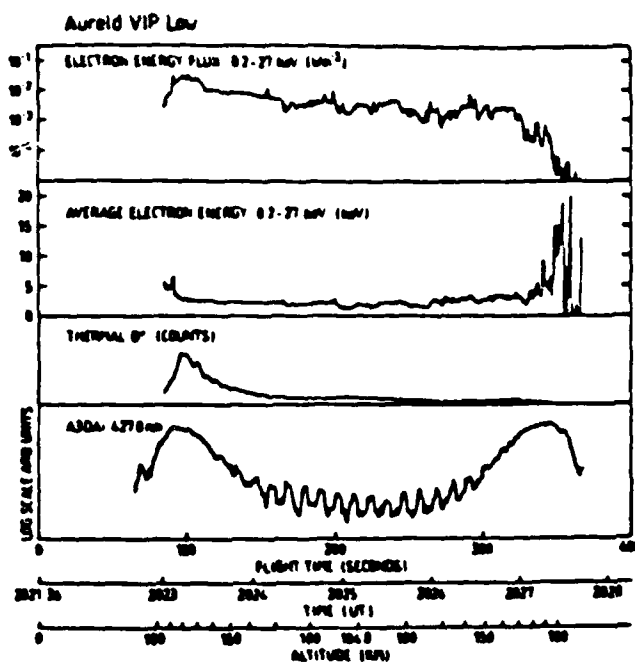


Figure 12





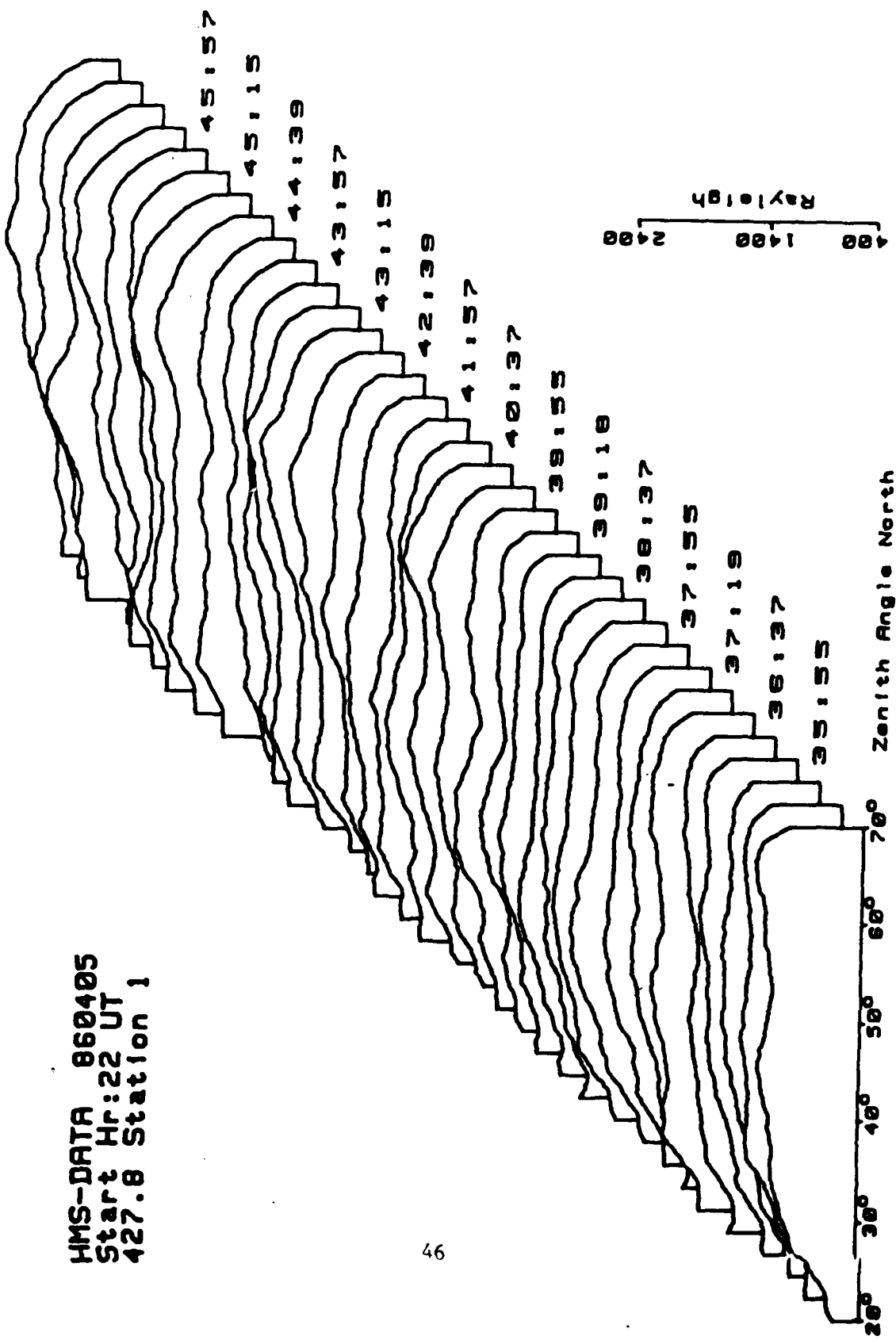
Summary plot of Aureld-VIP-Low data. The panels show from top to bottom: the electron energy flux, the average electron energy, the relative intensity of thermal O<sup>+</sup> ions, and the intensity of the 427.8 nm emission, measured perpendicular to the rocket spin axis in the south direction.

A closer look on the period 2235-2312 UT on April 5, 1986 using the HMS-station at KGI. Data has been fully corrected (extinction, van Rhijn and background) and is low-pass filtered. Scale is given in absolute intensities. The times for the four VIKING images in Fig. 6 are indicated.

a-c: 427.8 nm, 20 s averages. Note that the baseline for each curve is 400 R.

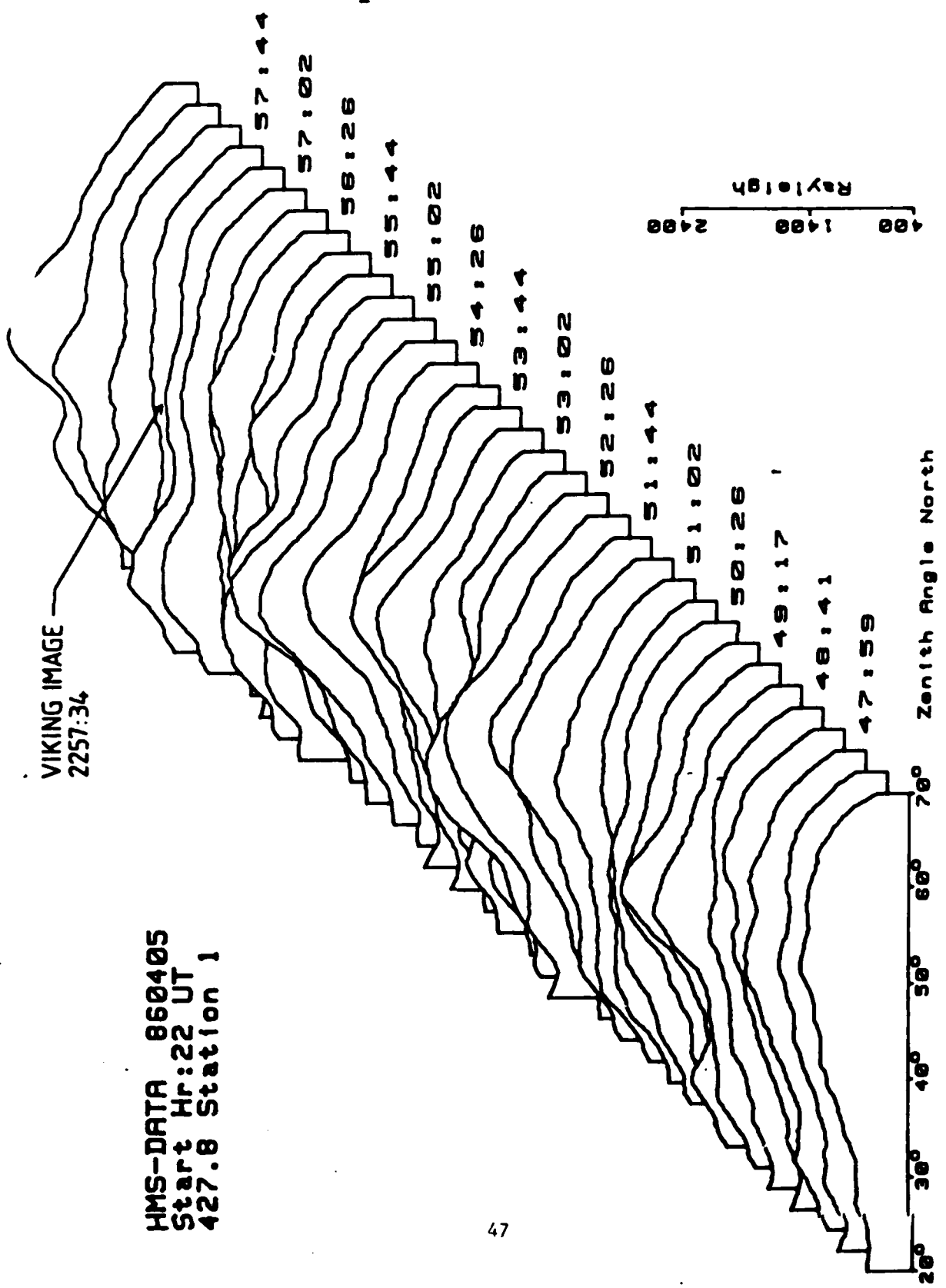
d: 630.0 nm, sampled every minute.

HHS-DATA 860405  
57847 H4:22 UT  
427-B State 10n 1

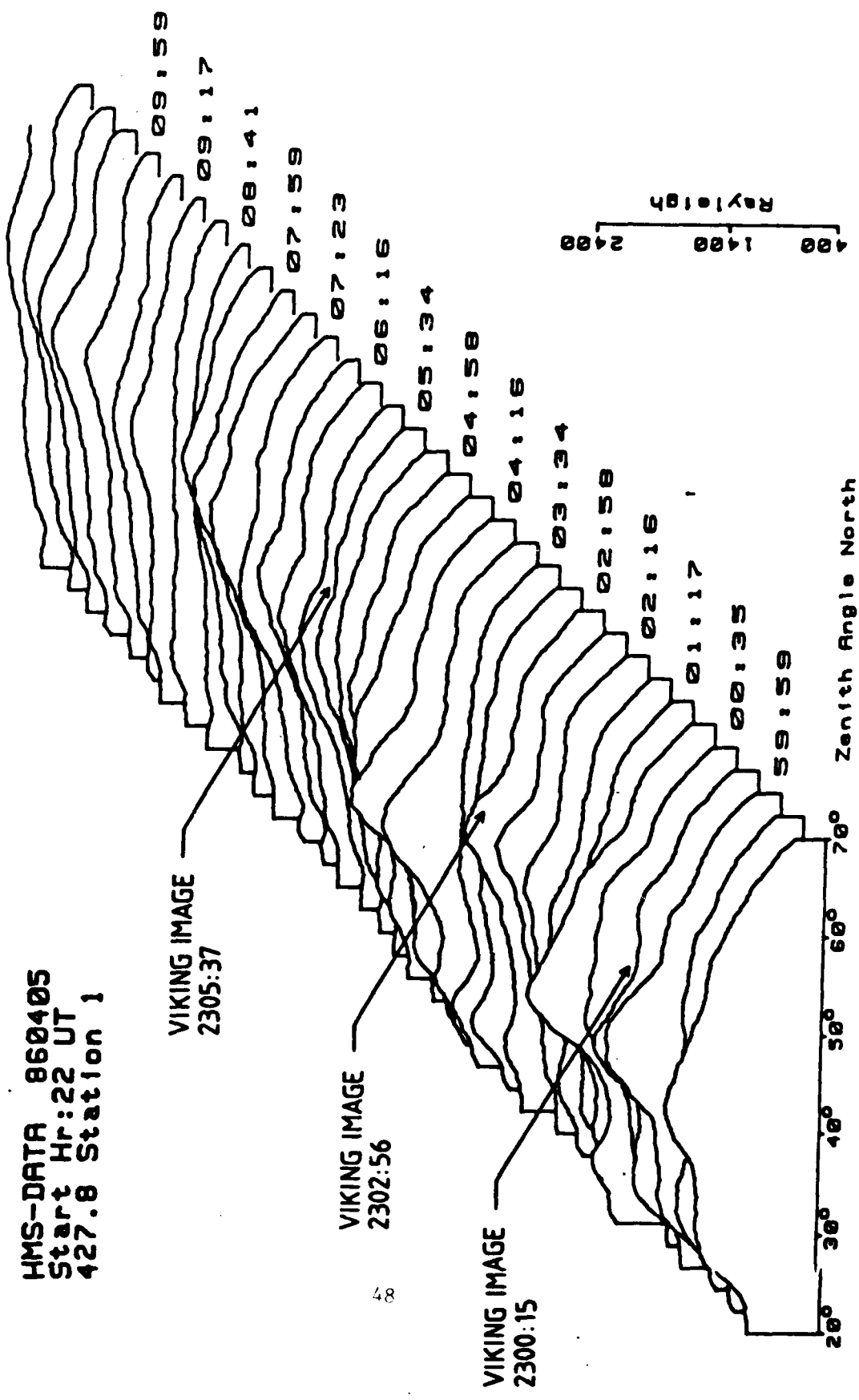


VIKING IMAGE  
2257:34

HMS-DATA 860405  
Start Hr:22 UT  
427.8 Station 1



HMS-DATA 860405  
Start Hr:22 UT  
427.8 Station 1



### A NEW FACILITY FOR OPTICAL AURORAL MEASUREMENTS

At the Swedish Institute of Space Physics, IRF, (Institutet för Rymdfysik, former name: Kiruna Geophysical Institute) in Kiruna, Sweden a new optical laboratory for auroral measurements has been taken into operation. Kiruna is an auroral station with geographic coordinates: 67.8°N, 20.4°E; dipole coordinates: 65.2°N, 116.0°E and L-value: 5.35. Kiruna can be reached several times a day with direct flights from the international airport outside Stockholm. The Institute is located quite near (8 km) to the town of Kiruna, providing good social services but also creating some man-made light which must be considered when certain optical measurements are carried out at the Institute.

Northern Scandinavia has experienced a growth of advanced scientific installations over the last 10 years. The area contains two rocket ranges (ESRANGE and ANDØYA), a tristatic and a monostatic incoherent scatter radar system (EISCAT) and a coherent radar system (STARE). Several other novel experiments can be found at observatories or observing sites at Spitzbergen, Skibotn, Kilpisjärvi, Sodankylä, Lycksele and Kiruna.

Optical measurements represent perhaps the oldest instrumental method in scientific auroral research, especially if the human eye is included. The importance of the method has recently increased due to the technological advancement in digital storage technology and as the result of new light sensitive detectors (e.g. CCDs).

The basic scientific motivation for an optical research program in the auroral zone is that the ionosphere displays through aeronomical processes the final result of plasma processes in the ionosphere and in the magnetosphere. The photon emitting auroral structures contain important information in their three-dimensional form, dynamical features and in the spectrum of the emitted light. No other method possesses the high resolution capabilities (both in time and space) as the optical measurement method.

To continue with the optical research program in Kiruna a major improvement in the experimental research facilities was necessary. We decided to build the new optical laboratory at the top of the main building of the Institute. The main building of the Institute is oriented almost in the geographic east-west direction. A row of domes along the roof will therefore have a clear field of view in the north-south direction. The horizontal roof of the new building (fig 1a) contains 7 large domes (1.0 m diam), and the 45° elevation roof facing geographic north has 6 smaller domes (0.6 m diam). In addition to the plexiglass domes, windowless openings are also available. The profile of the roof was chosen to make the removal of snow and ice easier. Normal snow precipitation is melted away by heating wires placed around the domes.

The new available working space was divided into 6 measurement rooms and a long common corridor (fig. 1b). The light sensitive instruments are placed in the measurement rooms. The personal computers and the data storage units are placed just outside the rooms in the corridor. Dimensions important for mounting considerations are common for all measurement rooms and can be found in fig. 1c. Each individual measurement room can be temperature stabilized from about +8°C up to +25°C. The plexiglass used for all domes has been chosen for its ability to transmit light in the UV-region. The domes give a 50 per cent transmission down to 280 nm.

The instruments in operation and the present area of scientific interest are found in table 1. The evolution of the optical research program in Kiruna has followed two lines: monochromatic imaging and measurement of the neutral wind (in collaboration with Dr. David Rees, UCL, London).

A more detailed description of the new optical laboratory is given in Ref. 1. The Institute welcomes guest scientists in optical auroral research.

TABLE 1: Ground-based optical research instrument in Kiruna

<u>Instrument</u>	<u>Description</u>	<u>Status</u>
Standard all-sky camera	16 mm colour film, 6 frames/min. Information on cloudiness and auroral activity.	routine operation
Auroral Dynamics Imaging System (ADIS)	A low light level TV-system. Monochromatic. 170° FoV. High time resolution auroral morphology.	operated during campaigns
Height Measuring System (HMS)	A bistatic system for triangulation of auroral heights in real time. One-dimensional intensified Reticon arrays. Gives also information on the intensity along the magnetic meridian.	routine operation
Meridian Measuring Array (MMA)	A thermoelectric cooled CCD-camera. Tektronix 512x512 thinned device. Digital optical disc used as a storage unit. High quality imaging of aurora.	Test operation during 1987.
Single FPI	Single-etalon Fabry-Perot Interferometer. Neutral wind and temperatures at 240 km altitude. 7 directions, 30 s integration time.	routine operation since 1980/81
Green line FPI	Single-etalon Fabry-Perot Interferometer. E-region meridional wind.	operated during campaigns
DIS	Doppler Imaging System, bistatic. monostatic: in Wind pattern over 800x800 km. 120° FoV. 5 min time resolution.	-operation, bistatic: start 1987.
Triple FPI	Triple-etalon Fabry-Perot Interferometer. Thermospheric winds during full daylight.	start during 1986/87. Permanent 12 months 1987.
Imaging spectrometer	12x20 cm grating (CZ-turner) Imaging photon detector. Up to 50 nm spectrum (0.2 nm res.) Imaging along meridian.	operated during campaigns

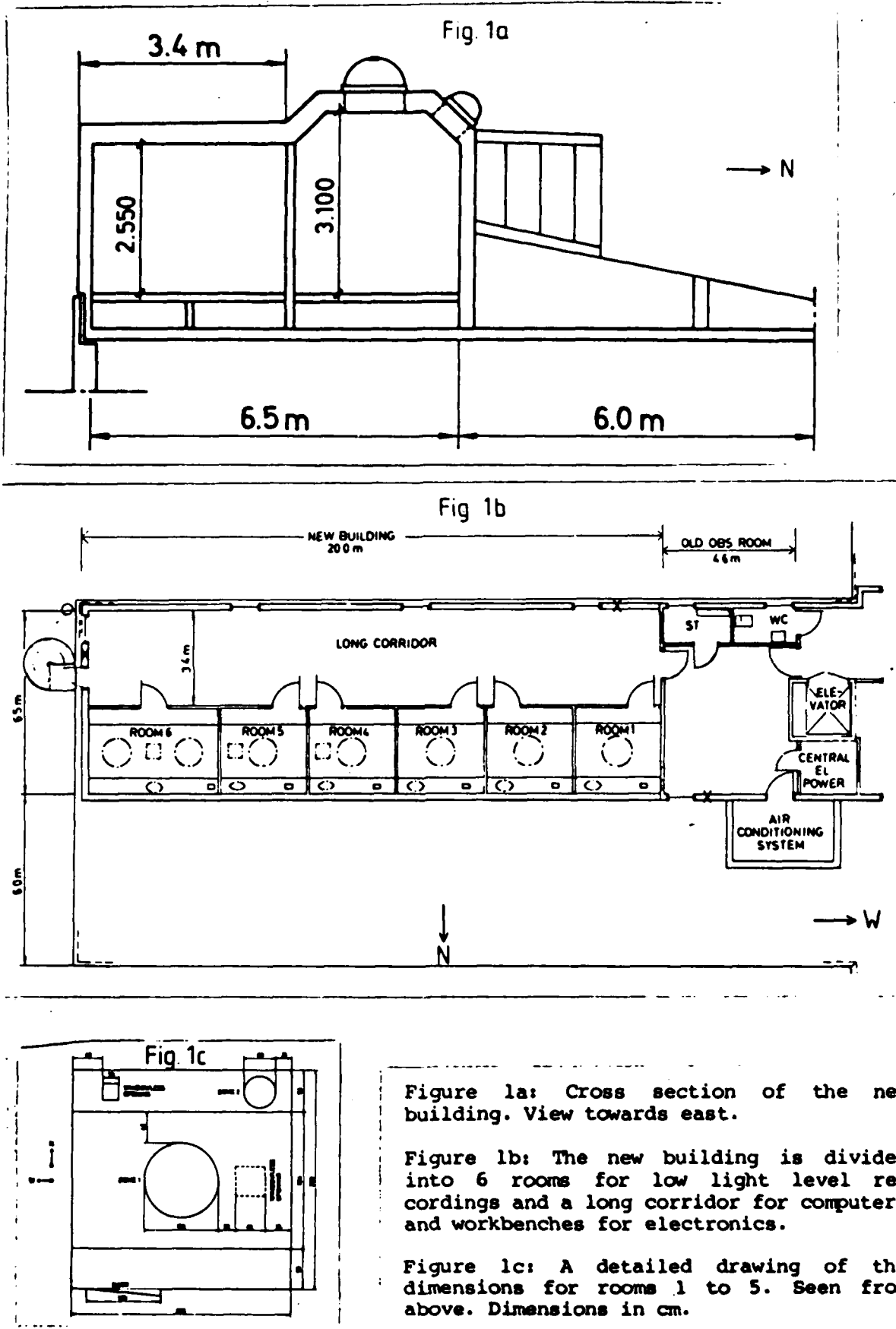


Figure 1a: Cross section of the new building. View towards east.

Figure 1b: The new building is divided into 6 rooms for low light level recordings and a long corridor for computers and workbenches for electronics.

Figure 1c: A detailed drawing of the dimensions for rooms 1 to 5. Seen from above. Dimensions in cm.

Åke Steen  
Swedish Institute of Space Physics  
P.O. Box 812  
S-981 28 Kiruna  
Sweden

References

Ref. 1: Steen, Å., The optical laboratory in Kiruna: a new research facility in the auroral zone, KGI Technical Report 033, February 1987.

E N D

DATE

FILMED

8 - 88

OTIC